EVALUATION OF ANNULAR PRESSURE BUILDUP (APB) DURING WCD BLOWOUT OF DEEPWATER HP/HT WELLS

A Thesis

by

MATIN TAGHIZADEH ANSARI

Submitted to the Office of Graduate and Professional Studies of
Texas A&M University
in partial fulfillment of the requirements for the degree of

MASTER OF SCIENCE

Chair of Committee,	Jerome Schubert
Committee Members,	Catalin Teodoriu
	Yuefeng Sun
Head of Department,	A. Daniel Hill

December 2014

Major Subject: Petroleum Engineering

ABSTRACT

Annulus Pressure Buildup (APB) is one of the major design considerations/problems for deepwater wells. APB is even more problematic in High Pressure/High Temperature (HP/HT) wells. High flow rates could potentially worsen the APB issue. Although conceptually APB is well understood, arriving at an acceptable prediction of its magnitude is challenging and requires a more subtle approach; such an approach would include utilization of appropriate transient multiphase flow and thermal models, in addition to proper handling of the PVT properties of the wellbore and annular fluids. To account for wellbore transient behavior during the Worst Case Discharge (WCD) blowout scenario, a transient multiphase flow model needs to be coupled with a robust transient tubular load/stress analysis model.

To date, there has not been a commercial software package that analyzes the dynamic interaction of fluid flow and tubular systems within a well. Hence, it is proposed herein to employ three independent industry-leading software packages to analyze the 1) fluids, 2) flow, and 3) tubulars, and integrate the outputs into a unified solution.

The proposed new methodology begins with flow dynamics such as pressure and temperature being coupled with the flowing fluid's PVT properties. Then, the interaction between the fluid's flowing pressure and temperature and the loads and stresses applied on the tubulars is analyzed. Finally, a Von Mises criterion is used to investigate the

wellbore integrity by taking the uniaxial, biaxial and triaxial limits, along with the design safety factors, into account.

Furthermore, the importance of the APB issue in a WCD scenario is highlighted with an example and a remedy, such as an alternative wellbore design.

In the absence of any published literature, guidelines, or software package that could properly analyze the transient effects of the fluid flow and tubular loads, implementation of the proposed new method/procedure could help to predict, identify and resolve potential well integrity issues.

ACKNOWLEDGEMENTS

I would like to thank my committee chair, Dr. Schubert, and my committee members, Dr. Teodoriu and Dr. Sun, for their guidance and support throughout the course of this research.

Thanks also go to my friends and colleagues and the department faculty and staff for making my time at Texas A&M University a great experience. I also want to extend my gratitude to Boots & Coots International.

I would like to give my special thanks to my dear husband for his support all along the way. Finally, thanks to my mother and father for their encouragement.

NOMENCLATURE

APB	Annular Pressure Buildup
P-T	Pressure-Temperature
WCD	Worst Case Discharge
BSEE	Bureau of Safety and Environmental Enforcement
FWHP	Flowing Well Head Pressure
FBHP	Flowing Bottom Hole Pressure
CGR	Condensate Gas Ratio
GLR	Gas Liquid Ratio
API	American Petroleum Association
SRK	Soave-Redlich-Kwong
VLE	Vapor-Liquid Equilibrium
PR	Peng-Robinson
GOR	Gas-Oil Ratio
P	Minimum Internal Yield Pressure
Y_{Pa}	Reduced Yield Strength of Axial Stress Equivalent Grade
S_a	Axial Stress
Y_p	Minimum Yield Strength
EoS	Equation of State
HPHT	High Pressure High Temperature
VME	Von Mises Equivalent

OD	Outer Diameter
ID	Inner Diameter
AFV	Annular Fluid Expansion
BOP	Blowout Preventer
σ_{VME}	Triaxial Stress
σ_z	Axial Stress
σ_θ	Tangential or Hoop Stress
σ_r	Radial Stress
PVT	Pressure-Volume-Temperature
TD	Total Depth
TVD	True Vertical Depth

TABLE OF CONTENTS

Page

Page

LIST OF FIGURES

Page

Page

LIST OF TABLES

Page

1 INTRODUCTION AND LITERATURE REVIEW

In deepwater wells, completion fluids are commonly trapped in casing annuli above the top of the cement and below the wellhead. Annular Pressure Buildup (APB) is pressure generated by the thermal expansion of fluids left in a sealed annular space. If the hot formation fluids flow to the seabed, the heat will be transferred to the surroundings via both conduction and convention. As a result, the trapped annular fluids heat up and expand in a closed system, which could increase the annular pressure by as much as 10,000 – 12,000 psi, according to Bloys et al. (2008). The over-pressurization of tubulars could result in events such as the Marlin A-2 incident in the Gulf of Mexico in November 1999, as discussed by Bradford et al. (2002).

In general, annulus integrity can be compromised in three ways:

1. Over-pressurizing the wellhead/hanger/casing above the maximum absolute pressure and temperature;
2. Exceeding the maximum burst pressure differential (outward); and
3. Exceeding the maximum collapse pressure differential (inward).

The physical mechanisms of APB are well understood, and theoretical models have been proposed and documented by several authors such as Klementich and Jellison (1986), Adams (1991), Adams and McEacharn (1994), and Halal and Mitchell (1994).

The potential negative effects of APB and consequent load stresses make vital the proper modeling of the complex temperature and pressure characteristics in the wellbore. Hence, the magnitude of the APB in one or more annuli should be formulated

such that the Pressure-Temperature (P-T) induced volume changes of the annular fluids relate to the P-T induced volume changes of the annuli. The interaction of multiple annuli together with the thermal expansion of the fluids, ballooning and compression of the tubulars, leak-off of annular fluids, and influx of formation fluids should all be taken into account.

While most available software packages such as WELLCAT™ are programmed to help with casing/tubing design during drilling or production, there has not been significant interest in the evaluation of APB during a blowout, capping and containment of the wellbore.

Since in a typical deepwater well the temperature at the top of ubsea annulus is ~40 ^{o}F, while the temperature at the bottom could be as high as 400 ^{o}F, the thermal properties of the fluid at the top can vary from the corresponding values at the bottom by as much as 10% for synthetic fluids. For water-based fluids, the difference can be even greater, according to Sathuvalli et al. (2005). Also, according to Kaarstad et al. (2008), laboratory measurements of drilling, completion, and packer fluids all showed that the actual compressibility values and expansion coefficients deviated significantly from the textbook values commonly used in the oil industry.

2 PROCEDURES/ METHODOLOGY

PVTsim, OLGA, and WELLCAT™ will be used in this research to analyze the fluid properties, flow conditions, and tubular stress loadings, respectively. The output of each model will be used as the input for the other model(s) in an iterative process.

PVTsim is a versatile PVT simulation program currently being used by leading oil producing and operating companies throughout the world. Based on extensive data collected over a period of more than 25 years, PVTsim is able to carry information from experimental PVT studies into simulation. The fluid parameters may be exported to produce high quality input data for other simulators. PVTsim will be used to determine the proper thermal fluid properties to be used in OLGA and WELLCAT™.

The OLGA dynamic multiphase flow simulator models time-dependent behaviors and transient flow. Transient simulations provide an added dimension to steady-state analyses by predicting system dynamics such as time-varying changes in flow rates, fluid compositions, pressure, and temperature. OLGA will be used to account for reservoir and flow dynamics. The estimated pressure and temperature profiles will be fed into PVTsim and WELLCAT™.

WELLCAT™ software provides precise solutions for both wellbore analysis and integrated casing and tubing design. The software calculates accurate downhole temperature and pressure profiles, which can then be used for pipe-body movement and casing and tubing load analysis. WELLCAT software is the tool of choice for many companies operating in high-pressure, high-temperature (HPHT) deepwater. Thermal

effects are modeled for a comprehensive analysis of loads and stresses on casing and tubing. Detailed analyses of the entire casing system are provided, in order to help researchers understand the effects of annular pressure buildup and interactions in the casing and tubing systems within a well. Loads and their resulting wellhead movement are evaluated to determine the integrity of the well tubulars. WELLCAT™ will be used to predict pressure and volume changes due to APB. The estimated pressure and temperature values will be input into PVTsim and OLGA.

3 TECHNICAL BASICS AND EQUATIONS

3.1 Wellbore Integrity

The exerted forces on a wellbore are mainly determined by pressure, weight, mechanical forces and friction. Equilibrium equations, coupled with elastic stress-strain relations, can be used to analyze thermal strain, buckling, axial strain (hoop stresses), and applied forces and loads.

To investigate wellbore integrity during a blowout, the wellbore flowing pressure profile must first be determined. Since the pressure predictions have a significant impact on temperature as well, choosing a proper flow model is critical to the accuracy of the predicted pressures in the wellbore.

3.2 Worst Case Discharge (WCD)

WCD is an estimate of the maximum potential flow rate of a well. For offshore wells, the WCD, as defined by the Bureau of Safety and Environmental Enforcement (BSEE), is the openhole (no drillstring in the hole) blowout to the seabed with full reservoir exposure and no flow restrictions. WCD analysis was mandated by the U.S. government in the aftermath of the Deepwater Horizon oil spill. WCD is calculated by linking a reservoir/inflow model to a nodal analysis model. Some commercial software packages currently available for use in calculating WCD include OLGA, PROSPER, GAP and Merlin.

3.3 Multi-Phase Flow

WELLCAT™ offers both steady-state correlation and mechanistic flow models, while OLGA is a transient multiphase flow simulator. The five correlation models are Beggs and Brill (1973), Orkiszewski (1967), Hagedorn and Brown (1965), Duns and Ros (1963), and Gray (1974); the three mechanistic models are Zhang et al. (2003), Kaya et al. (1999), and Ansari et al. (1994).

3.3.1 Steady-state Correlation Models

Selection of the flow model should be based on the type of produced fluid and inclination of the wellbore, as shown in **Table 3.1**.

Table 3.1– Comparison of steady-state correlation models

Fluid	Factors	Recommended Correlation
Oil	High Deviation (>50)	Beggs & Brill
	High Gas/Liquid Ratio	Duns & Ros, Orkiszewski
	Low GLR or High Water Cut	Hagedorn & Brown, Orkiszewski
Gas	Dry Gas (no liquids)	All models
	High Deviation	Beggs & Brill
	Low GLR/High Water Cut	Hagedorn & Brown
	Some liquid (Low CGR)	Gray

The Orkiszewski correlation is comprised of three other correlations for different flow regimes of:

- Bubble flow (mostly liquid with small gas bubbles present): Griffith and Wallis
- Slug flow (gas phase is more pronounced, but the liquid still dominates): Hagedorn and Brown
- Mist flow (mostly gas with liquid condensate): Duns and Ros

Hence, if the behavior of the liquid is expected to vary throughout the wellbore, it is recommended to use the Orkiszewski correlation.

Choosing a proper two-phase correlation is highly case-sensitive, and a comprehensive sensitivity analysis should be carried out to validate the chosen model with the flowing fluid's pressures and temperatures, when available.

3.3.2 Steady-State Mechanistic Models

In mechanistic models, a simple correlation such as Barnea et al. (1980) is first used to determine the flow pattern. Common flow patterns include bubble, dispersed bubble, stratified, annular, and slug flow. Then, flow pattern-specific momentum equations are used to calculate multiphase flow behavior. These momentum equations require additional equations which are known as closure equations. Closure equations rely on physical conditions such as equality of pressure gradients and pressure-shear stress balances across the phase interfaces. Appropriate published models or correlations then determine the frictional shear stress in each phase, based on transition criteria

defined by analytic considerations, experimental correlations, or some combination of the two. Description of each model is explained in **Table 3.2**.

Table 3.2– Comparison of steady-state mechanistic models

Model	Description
Ansari	This model is intended mostly for upward flow in vertical wells with a deviation of up to 15 degrees, and considers six flow patterns: liquid, gas, bubble, slug, dispersed bubble, and annular flow.
Kaya	This model is applicable to angles of inclination up to 75 degrees, and considers ten flow patterns: liquid, gas, annular, slug, dispersed bubble, bubbly, churn, stratified way, stratified smooth, and elongated bubble flow.
Zhang	This model is applicable for both upward and downward flows in all inclinations and considers seven flow patterns: liquid, gas, dispersed bubble, annular, bubbly, intermittent, and stratified. The predicted pressure drop and liquid holdup calculated by the Zhang Unified model is found to be within a 15% error when compared with experimental measurements.

3.3.3 Transient Experimental Models

OLGA is the only commercially available transient multiphase flow simulator. The transient nature of OLGA offers an additional component to steady-state models by

taking time-dependent variables such as velocity, fluid composition, temperature and operational changes into account. The OLGA code has been verified through large-scale lab research testing and actual production data since the 1980s, and has become the industry standard for modeling flow dynamics.

3.3.4 Comparison of the Models

The steady-state models need a boundary condition; hence, either the pressure at the inflow (perforations) or the outflow (wellhead) needs to be defined. If the pressure at the wellhead is defined then the pressure at the perforations will be calculated, and vice versa. In the case of a discharge to the seabed, the Flowing Well Head Pressure (FWHP) will be equal to the seawater hydrostatic pressure of the wellhead. The Flowing Bottom Hole Pressure (FBHP) at the perforations, however, needs to be determined through nodal analysis.

The FBHP and FWHP, along with the oil and gas discharge rates, are determined based on the nodal analysis described in Appendix A. With the seabed hydrostatic pressure defined as the outflow boundary (FWHP), the flowing pressure profile during a blowout is calculated through different models; the results are presented in Figure 3.1.

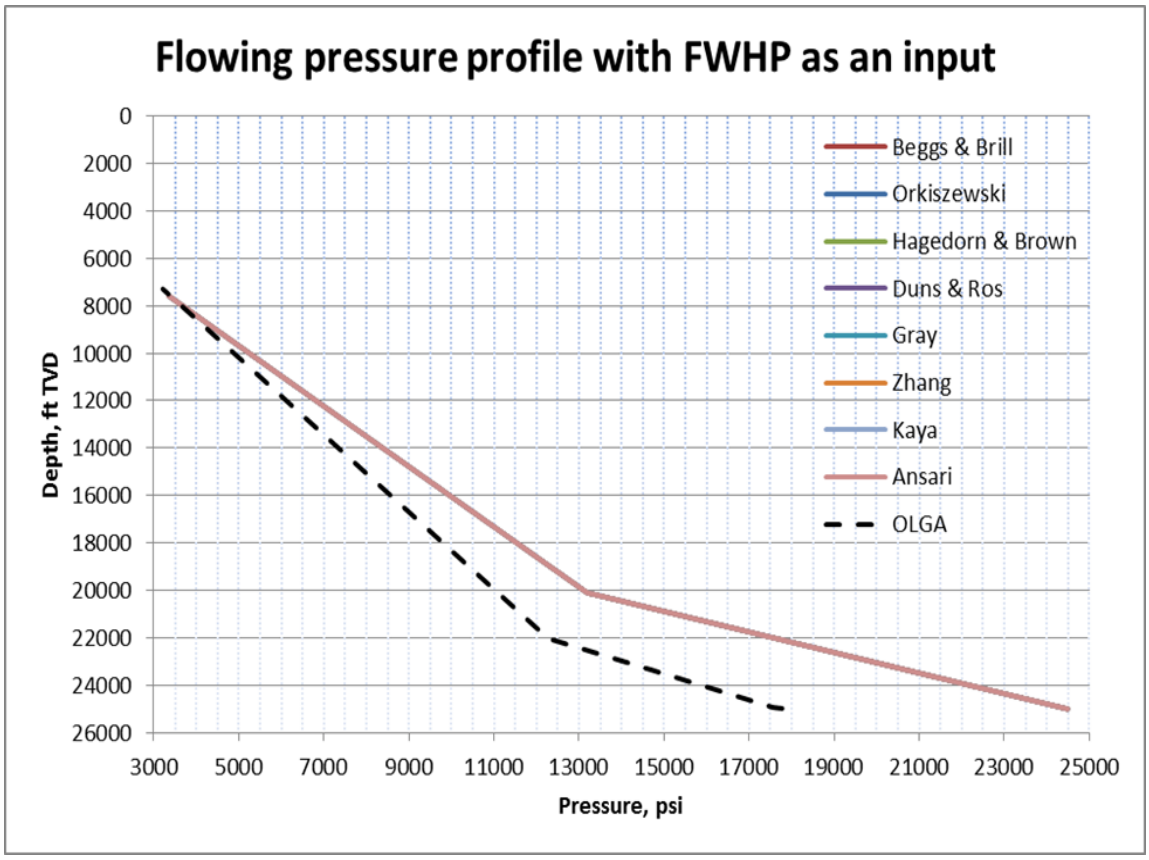

Figure 3.1– Comparison of predicted flowing pressure profiles with FWHP as an input along the wellbore during a blowout by different flow models

As shown above, with a defined FWHP, all the steady-state models predict the same pressure profile. Alternatively, if the FBHP (calculated by OLGA) is used as the inflow boundary at the perforations, then (as shown in **Figure 3.2)** the pressure profiles will differ.

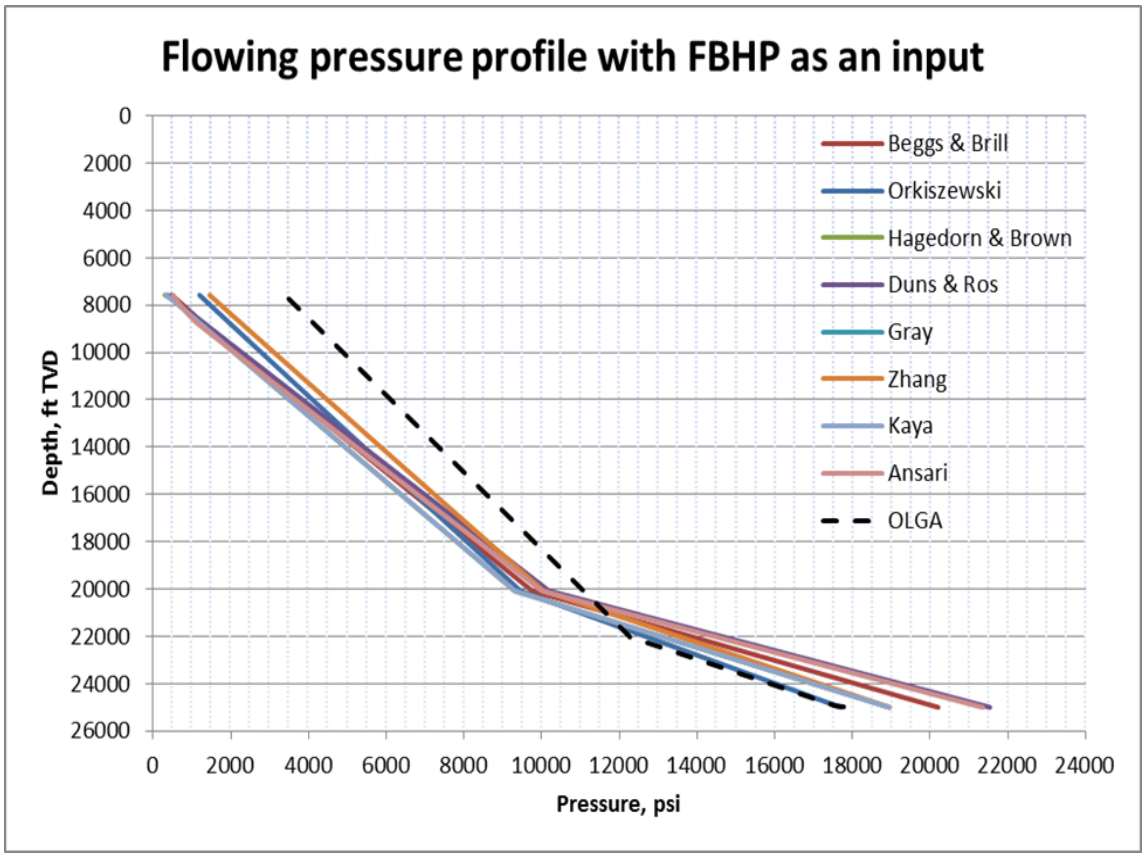

Figure 3.2– Comparison of predicted flowing pressure profiles with FBHP as an input along the wellbore during a blowout by different flow models

In this study, OLGA was chosen as the preferred flow model. Hence, the flow variables in the appropriate WELLCAT^{TM} flow model are manipulated to match the pressure profile predicted by OLGA.

3.4 Fluid Properties

In addition to the flow model, the flowing fluid's properties have a significant effect on the pressure and temperature calculations.

WELLCAT™ models any standard hydrocarbons composed of dry or free gas, oil and dissolved gas, vapor-liquids without heavy oil, and dissolved gas. The oil properties can be calculated by oil API gravity, while gas properties are modeled using the Soave-Redlich-Kwong (SRK)(1972) Equation of State (EoS).

In the case of condensate fluids, the Vapor-Liquid Equilibrium (VLE) compositional model gives more accurate gas and liquid densities at different temperatures and pressures, which has a significant effect on both the temperature and pressure predictions.

The Peng-Robinson (PR)(1976) Equation of State is used to calculate the fluid properties. Hydrocarbons of C7 and higher should be combined together into several heavy components. The molecular weight for these heavy components must be specified; however, the specific gravity is optional. The program will then compute typical values based on the molecular weight specified. Only three heavy components can be defined in the composition; thus, the heavy components will be lumped into three equivalent pseudo-components before being used in the calculations. Also, the molecular weight of C7 (101.205) through C10 (142.286) cannot be specified outside the defined range.

When an operation is defined, the gas and oil rates in the standard conditions should also be specified. If this results in a gas-oil ratio (GOR) that is different from that which was determined by the compositional model, the program will honor the input oil rate but use a new gas rate that honors the calculated GOR value. It should be noted that if the difference between the calculated and input GORs are within 5%, then no warning

will be issued and the input GOR will be used for the calculations. However, if the difference is more than 5%, then a warning will be issued and the input GOR will be changed to the calculated GOR.

The VLE flash calculations and thermal analysis must begin with an initial guess for the phase partition at the target pressure and temperature, which is obtained by interpolating between the nearest four points on the phase diagram. If the phase diagram is successfully calculated, the flash calculations and, thus, the resulting solution will be accurate. On the contrary, if the phase diagram is not accurately developed, the solution may not converge and the calculated fluid properties will have a high degree of uncertainty.

When the VLE diagram calculated by WELLCAT^{TM} does not suit the given fluid composition, a commercial PVT package such as PVTsim should be used to calculate the fluid properties.

PVTsim is a flexible Equation of State (EoS) modeling software package which can simulate the fluid properties and experimental PVT data. The fluid components can be characterized up to C80. The C7+ components can be lumped into pseudo-components. Nine variations of the Peng-Robinson (PR) and Soave-Redlich-Kwong (SRK) are offered to characterize the fluid properties.

In WELLCAT^{TM} the predicted pressure profile can significantly vary based on the type of fluid model used. Utilizing the fluid composition described in Appendix B, three types of fluid models are used in two different scenarios to highlight the various issues.

First, **Figure 3.3** shows a case involving a known FWHP, in which predicted pressure profiles by standard hydrocarbon model, VLE model, and imported PVTsim-characterized fluid are compared.

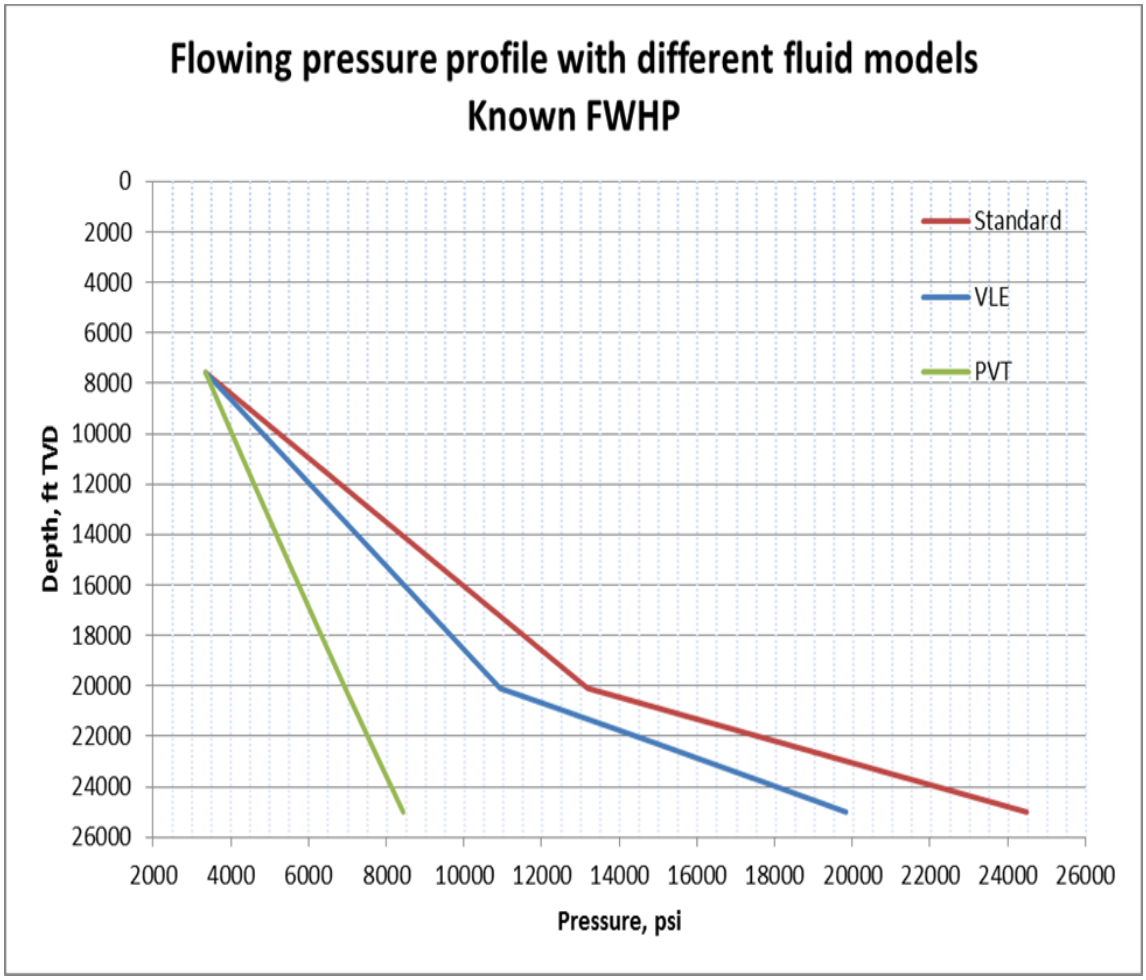

Figure 3.3– Comparison of predicted flowing pressure profiles with known FWHP along the wellbore during a blowout by different fluid models

A major problem with the standard hydrocarbon model is that the average molecular weight of the C7+ components cannot exceed 142.3; thus, the calculated properties do not match the laboratory measurements. The fluid properties of the imported PVTsim fluid are characterized by the PR78-Peneloux, which takes the volume corrections into the account (best match with the lab data). However, because of an issue in the WELLCAT^{TM} code, the flow will be choked and the rate reduced when using the imported file. Finally, the issue with the VLE model is that because of the type of EoS used, the calculated GOR and saturation points differ from the actual values by more than 25%.

Moreover, when the FBHP is known, neither model calculates the correct wellhead pressure (see **Figure 3.4**). In the case of a standard hydrocarbon, the defined FBHP had to be increased to yield a solution to the equations.

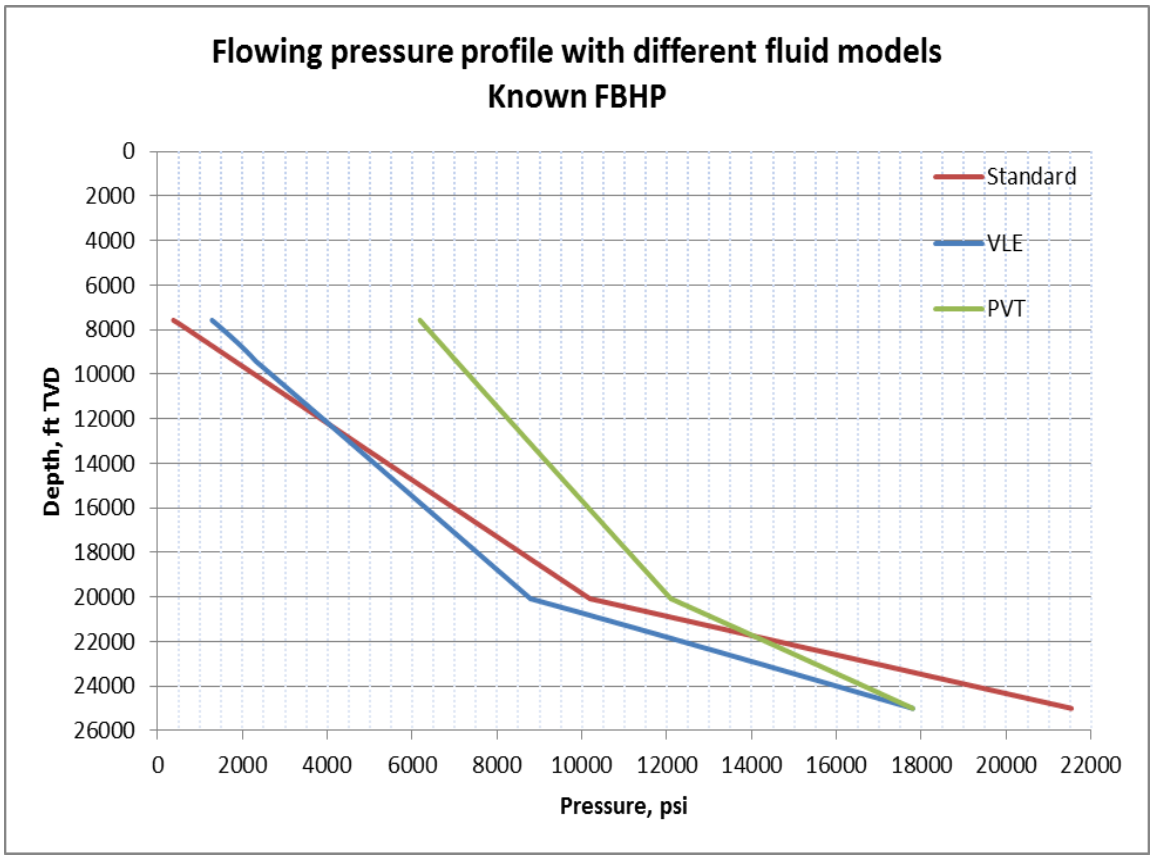

Figure 3.4– Comparison of predicted flowing pressure profiles with known FBHP along the wellbore during a blowout by different fluid models

In this study, the following approach is adopted to resolve these issues:

1. Using PVTsim, the fluid is characterized with the proper EoS.
2. The characterized fluid is re-characterized through a regression analysis to fit the EoS recognized by WELLCAT™.
3. The heavy components of the re-characterized fluid are lumped into pseudo-components that can be used in the WELLCAT™'s VLE hydrocarbon model.

3.5 Stress Analysis

In the stress analysis, since the application of the friction load requires a knowledge of the incremental displacement direction and the fact that numerical integration solutions need boundary conditions, the axial forces are determined based on the displacement instead of the seemingly-easier force equations. The displacement analysis is also used to compute the curvature and torque at any point in the string. Note that with no axial displacement in the cemented sections of the casing, the axial loads are ignored. Finally, the wellbore curvature, temperature changes, and internal-external pressures define the load conditions for the stress analysis.

3.5.1 Collapse

Collapse strength is mainly a function of the material's yield strength, and its behavior cannot be modeled by analytical yield or elastic collapse equations. The allowable stress under compression depends upon the slenderness ratio, D/t, and can be divided into three regions (as shown in **Figure 3.5)**. The short region is dominated by the strength limit of the material, while the intermediate (plastic) region is bounded by the inelastic limit. The long (elastic) region is constrained by the elastic limit.

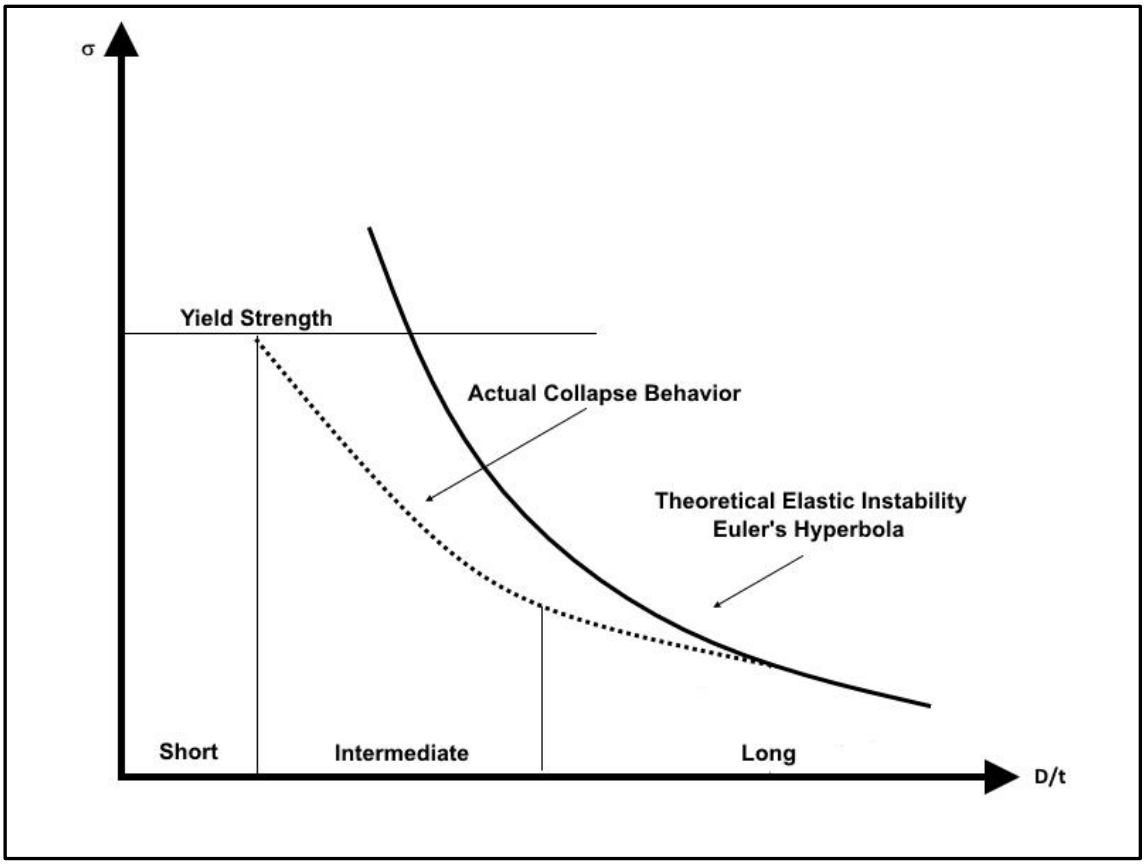

Figure 3.5– Collapse strength as a function of the D/t diagram

The collapse resistance of the material is primarily a function of its slenderness ratio (the ratio of the height or length and width or thickness, D/t) and API yield strength. Some other factors such as the shape of the stress/strain curve, ovality, residual stress, and eccentricity also affect the collapse strength.

The effect of tension loading on collapse strength is biaxial, and according to API Bulletin 5C3 (1985), can be expressed as follows:

$$Y_{Pa} = \left[\sqrt{1 - 0.75\left(\frac{S_a}{Y_P} \right)^2} - 0.5 \frac{S_a}{Y_P} \right] Y_P \quad , \quad \text{.....(3.1)}$$

Where:

P = minimum internal yield pressure, psi

Y_{Pa} = reduced yield strength of axial stress, psi

S_a = axial stress on the buoyant weight of pipe, lb_f

Y_p = minimum yield strength (yield point), psi

The reduced yield strength equation is based on the Hencky-von Mises maximum strain energy of distortion theory of yielding or triaxial analysis, which ignores radial stress and only applies to elastic yield failure. This tends to be a conservative assumption. The API collapse rating does not increase with compression.

3.5.2 Burst

For an ideal elastic-plastic material, the yield strength is defined as the stress at which plastic behavior begins. For tubulars, the yield strength is the maximum strength of the material at which the failure happens. The yield strength can be affected by high temperatures.

During tensile testing (as shown in **Figure 3.6)**, the onset of yielding occurs when the axial stress reaches the yield strength.

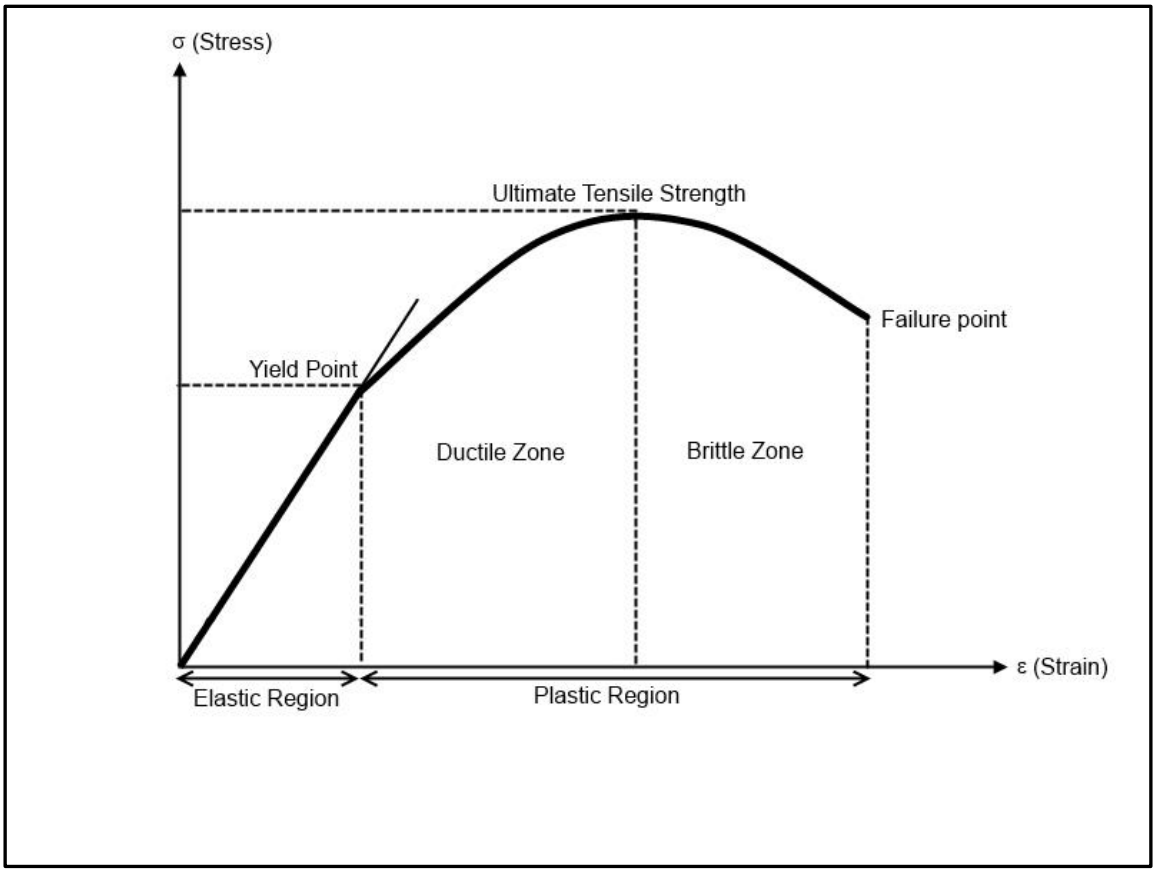

Figure 3.6– Strain/Stress behavior diagram

Since actual material failure is not imminent until the stress reaches the ultimate tensile strength, use of yield strength as the maximum allowable stress is an inherently conservative assumption.

3.5.3 Triaxial Analysis

The triaxial stress is a theoretical generalized three-dimensional stress state which combines the effects of all the principal stresses and then compares them with a uniaxial failure criterion (yield strength). The triaxial stress is also called the Von Mises

Equivalent (VME) stress. A yield failure can be identified when the VME exceeds the yield strength. Crandall and Dahl (1959) express the VME equation as follows:

$$Y_P \geq \sigma_{VME} = \frac{1}{\sqrt{2}}\left[(\sigma_z - \sigma_\theta)^2 + (\sigma_\theta - \sigma_r)^2 + (\sigma_r - \sigma_z)^2\right]^{\frac{1}{2}}, \quad \text{.....(3.2)}$$

Where:

Y_P = minimum yield strength, lb_f

σ_{VME} = triaxial stress, lb_f

σ_z = axial stress, lb_f

σ_θ = tangential or hoop stress, lb_f

σ_r = radial stress, lb_f

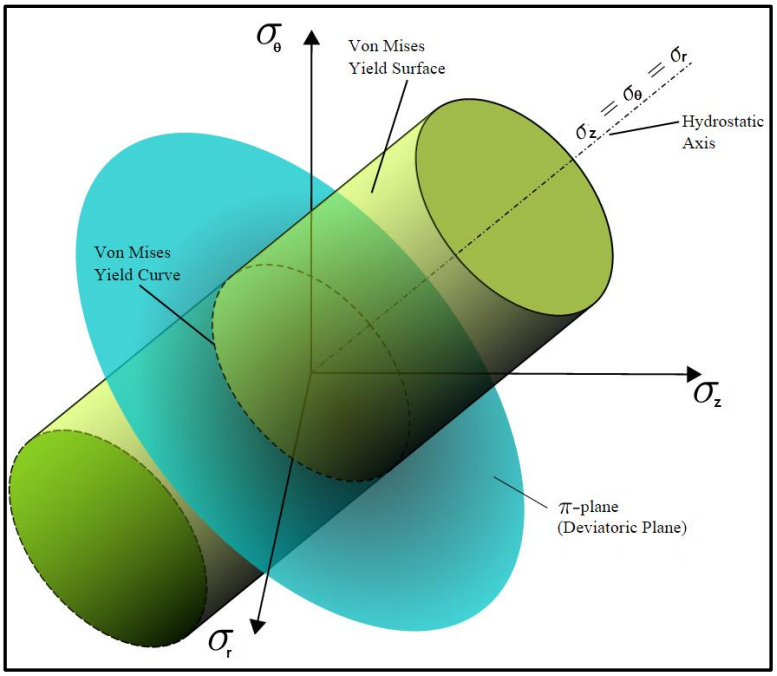

Figure 3.7 – Von Mises stress vectors (courtesy of Wikipedia)

The Von Mises stress factors are shown in **Figure 3.7**. Assuming a biaxial criterion with both σz and σθ >> σr and setting the triaxial stress equal to the yield strength, the equation of an ellipse can be written as:

$$Y_p = \left[\sigma_z^2 - \sigma_z\sigma_\theta + \sigma_\theta^2\right]^{\frac{1}{2}}, \quad \text{.....} (3.3)$$

A triaxial analysis could potentially account for the large temperature effects on the axial load profile in High Pressure High Temperature (HPHT) wells. This is

particularly important in combined burst and compression loading. Also, it could accurately determine stresses when using thick-wall pipe (D/t < 12).

The above equation accounts for both the effect of tension on collapse and axial load on API burst resistance. As shown by **Figure 3.8**, by plotting the ellipse, the triaxial criterion can be compared to the API ratings, and the loads which fall within the design envelope can be recognized as meeting the design criteria.

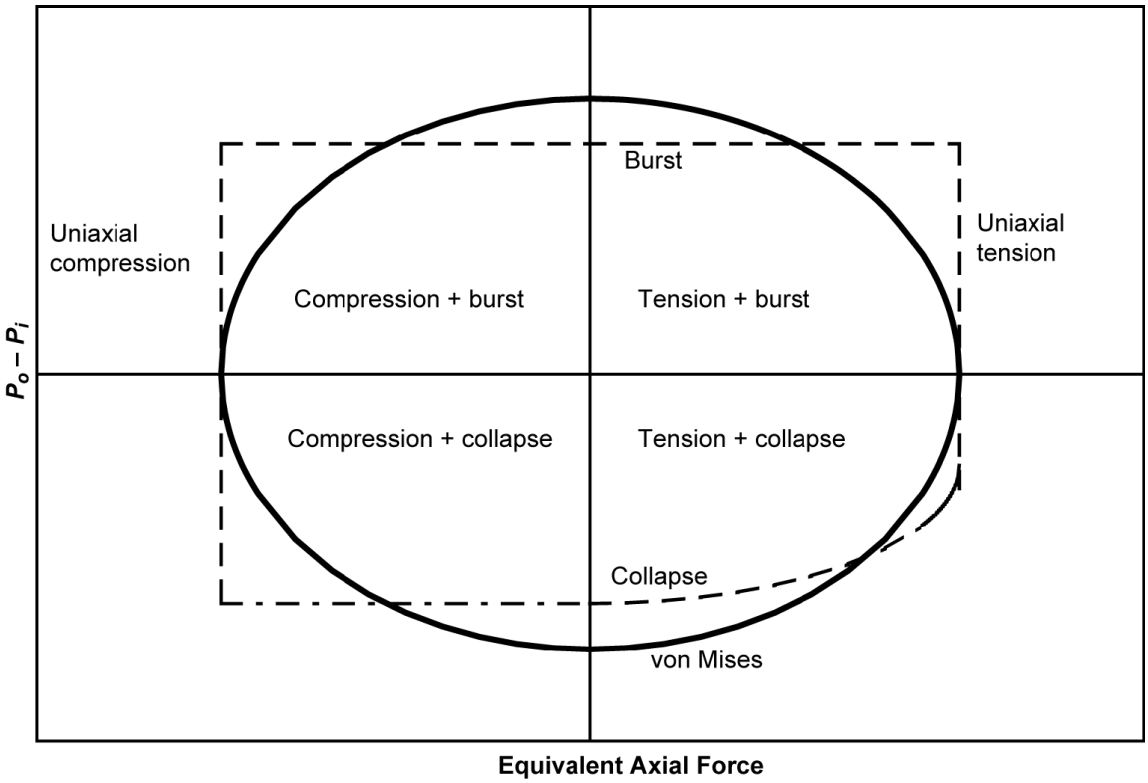

Figure 3.8 –Von Mises design envelope (courtesy of Petrowiki.org)

3.6 Safety Factors

In a stress analysis, the rating or allowable value is divided by the load or stress in the string. Safety factors for tension, burst, collapse, and triaxial stress are considered in the stress analysis. For instance, the axial safety factor is defined as the ratio of the tensile rating of the pipe and connector (the minimum of the pipe yield strength in tension and the connector tensile strength) to the computed effective axial force (the sum of the actual axial force and the maximum bending stress, developed by buckling, times the cross-sectional area).

3.6.1 Burst

The burst safety factor is defined as the ratio of the minimum of the pipe internal yield pressure, the connection internal yield pressure, and the connection leak pressure to the differential pressure.

3.6.2 Collapse

The collapse safety factor is defined as the ratio of the API collapse rating to the external pressure equivalent, which is a function of external and internal pressures.

3.6.3 Triaxial

The triaxial safety factor is defined as the ratio of yield strength to the Von Mises equivalent stress (axial, radial, hoop, and torsional shear stresses). To account for the worst case stress conditions, the axial stress is calculated with both compressive and tensile bending stresses. The Lame' formulas are used to determine the hoop and radial

stresses at the OD and ID. Finally, the shear stress is determined based on the torque induced by buckling.

Figure 3.9 graphically summarizes the uniaxial, biaxial and triaxial limits and design safety factors that need to be considered in the casing design.

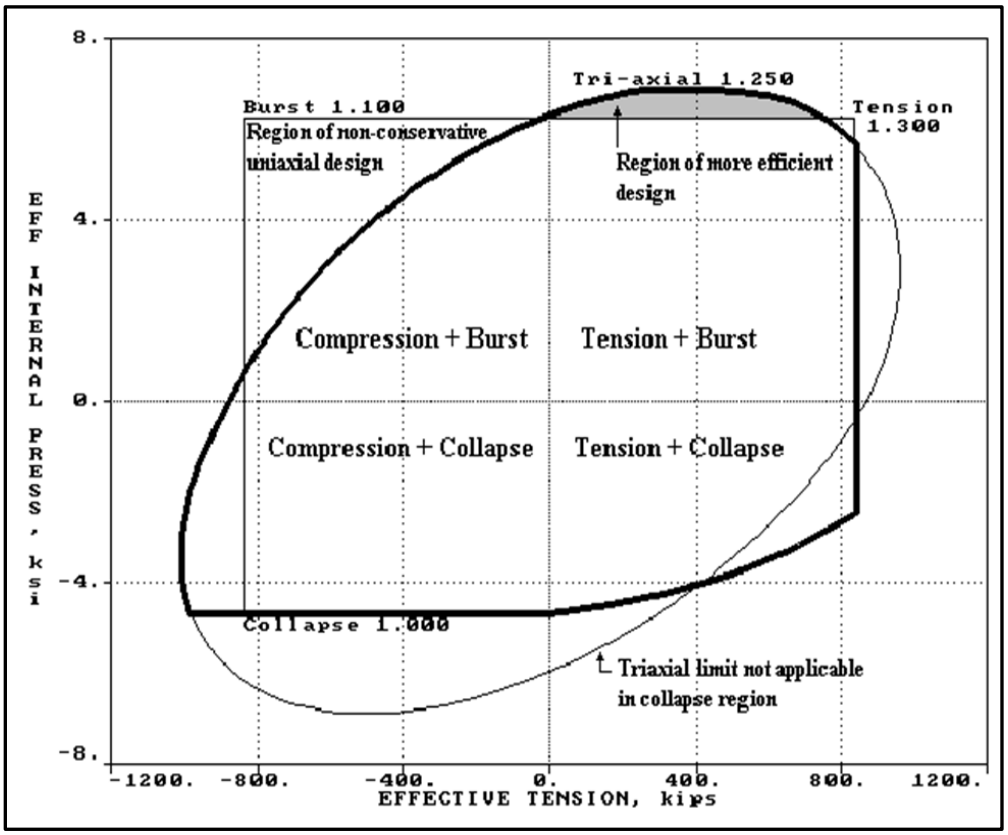

Figure 3.9 – Example of uniaxial, biaxial and triaxial limits and design safety factors (courtesy of Landmark)

In the next chapter, the well integrity during a WCD blowout will be evaluated.

4 CASE ANALYSIS

4.1 Case History

In this chapter, a wellbore design is presented and wellbore integrity during a WCD blowout is investigated (both WCD and restricted flow scenarios are described in Appendix A). A stress analysis is carried out, and after taking the triaxial, uniaxial and biaxial limits and design safety factors into account, the burst, collapse and APB criteria are examined. The resulting differential pressure between the strings is taken into the account to investigate the integrity of each individual string and its interaction with the other strings during both the WCD and the restricted flow. Subsequently, an alternate wellbore design is suggested to mitigate potential problems.

For the wellbore presented in **Figure 4.1**, the methodology described in the previous chapter is followed to achieve accurate flowing pressure and temperature profiles throughout the wellbore.

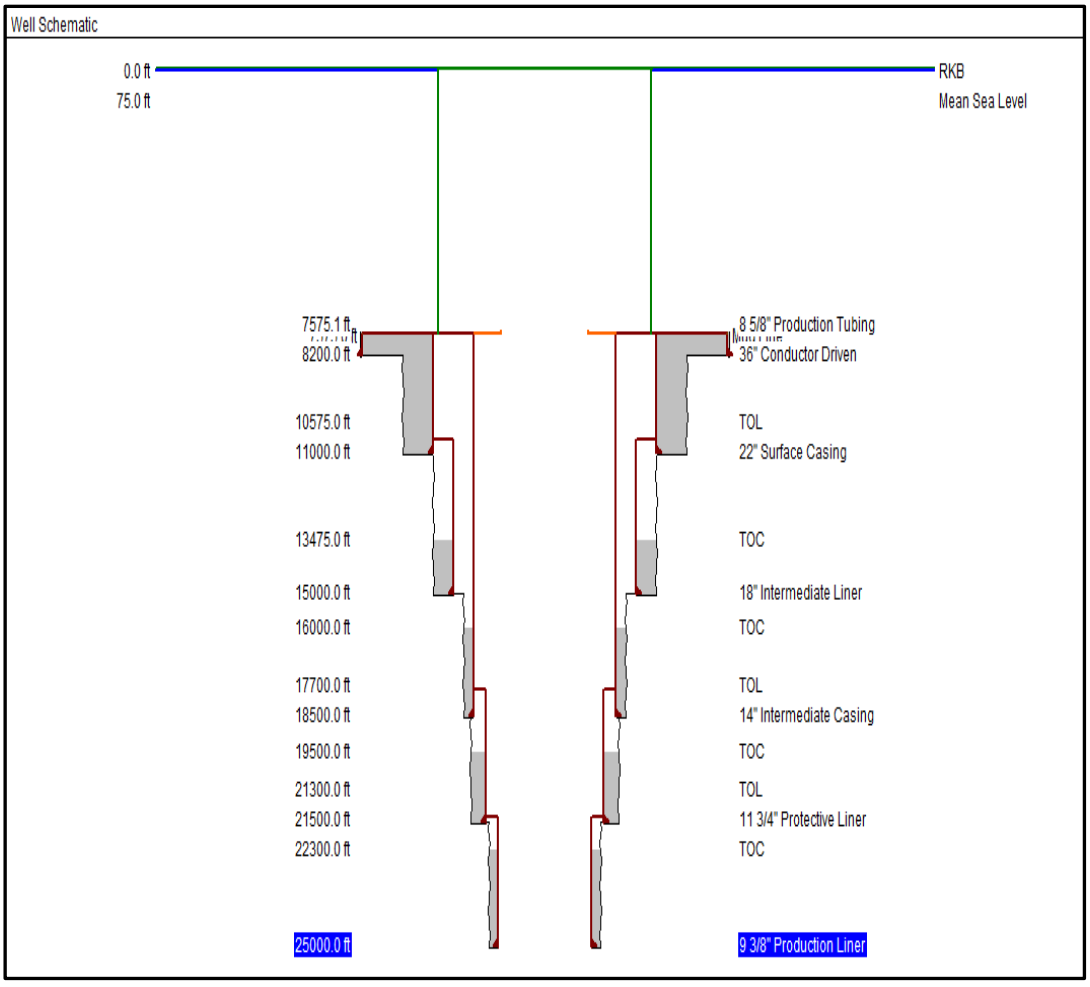

Figure 4.1 - Wellbore schematic

To signify the importance of analyzing the wellbore integrity during a WCD blowout versus a restricted flow, the flowing fluid's temperature is calculated in both cases. As **Figure 4.2** indicates, during the WCD blowout the fluid's temperature increases along the wellbore, while at a low rate it decreases. This increase in temperature could potentially lead to 1) significant annular pressure buildup which could

compromise the wellbore integrity, and 2) failure of equipment such as the wellhead, BOP, hanger seals, etc.

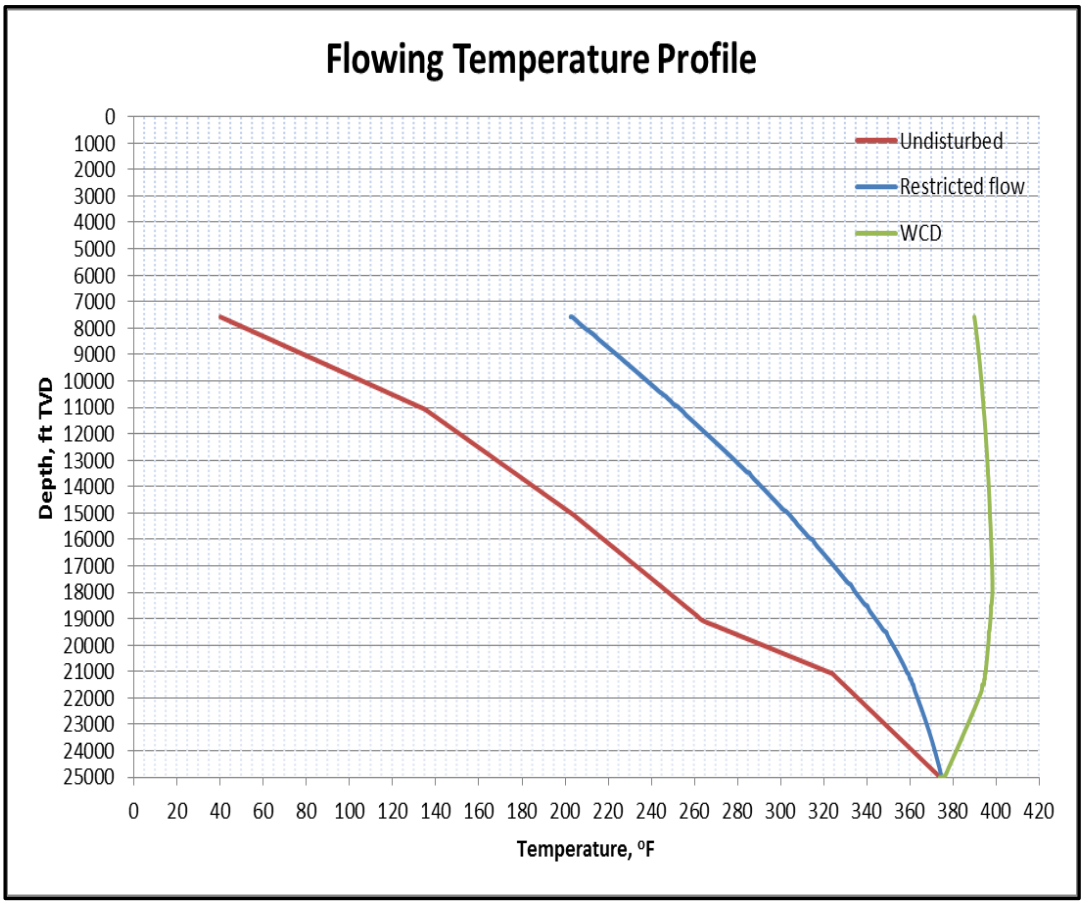

Figure 4.2 – Comparison of flowing fluid temperatures in restricted flow and WCD scenarios

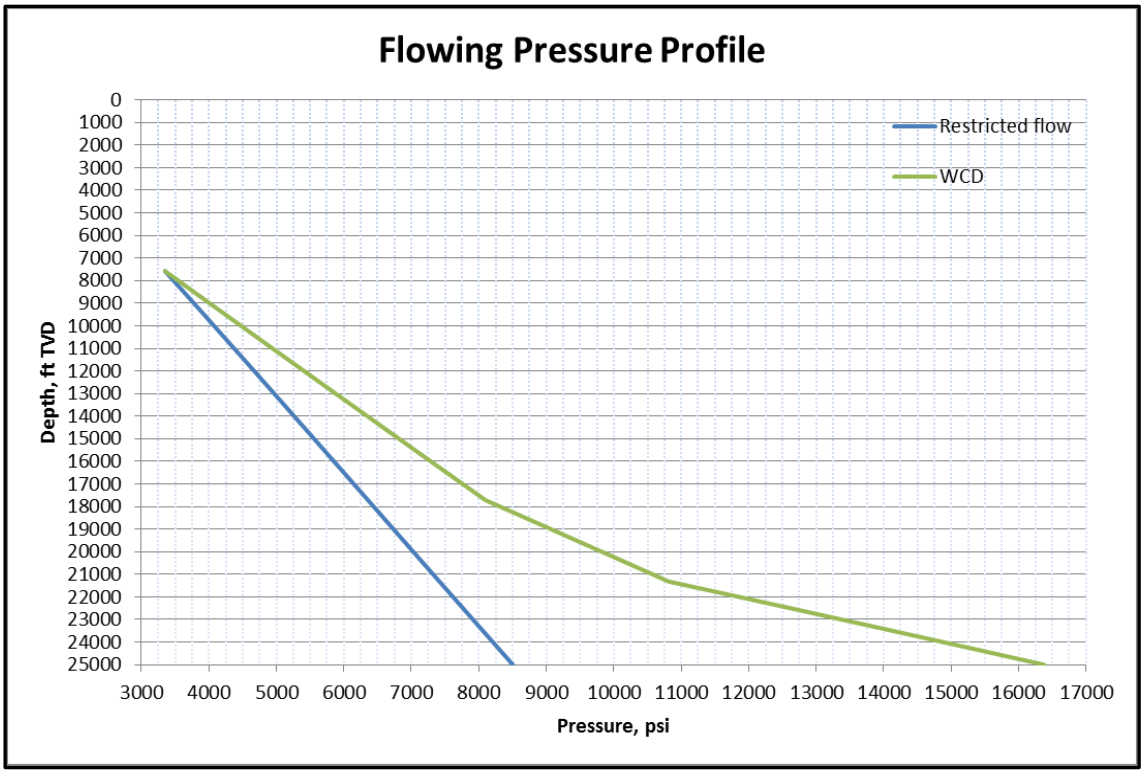

Figure 4.3 – Comparison of flowing fluid pressures in restricted flow and WCD scenarios

As shown in **Figure 4.3**, when producing at a high rate, the wellbore pressure profile is considerably different from when producing at a low rate. The higher pressure profile, in addition to the higher temperature profile, makes consideration of a WCD stress analysis crucial to a well design.

Table 4.1 shows the multi-string Annular Fluid Expansion (AFE) summary for each case.

Table 4.1– Comparison of Annular Fluid Expansions (AFEs) in restricted flow and WCD scenarios

Case	String Annulus	Incremental AFE Volume, bbl	Incremental AFE Pressure No leak-off, psi	Incremental AFE Pressure With Leak-off, psi
WCD	18" Intermediate Liner	39	13,331	1,768
	14" Intermediate Casing	94	13,998	2,537
	11 3/4" Protective Liner	4.4	6,991	2,074
Restricted flow	18" Intermediate Liner	18.2	6,432	1,768
	14" Intermediate Casing	38.7	6,263	2,537
	11 3/4" Protective Liner	2.6	4,180	2,074

The incremental AFE volume is the volume change caused solely by the AFE effect, and the incremental AFE pressure is the pressure change caused solely by the AFE phenomenon. It is clear that when the trapped annular fluid is able to leak off into the formation, the APB is much less of a problem. However, leak-off could be minimized or stopped because of deposition of the solid particles, plasticity of salt formations, etc. Incidents like the Marlin A-2 well are perfect examples of such cases. Also, it has been observed that the point loading exerted by the inward collapse of an outer string could cause the collapse of the inner string(s).

4.2 Stress Analysis and Wellbore Integrity

In this section, the design limits of each string for cases both of restricted flow and WCD are examined.

4.2.1 Restricted Flow Scenario

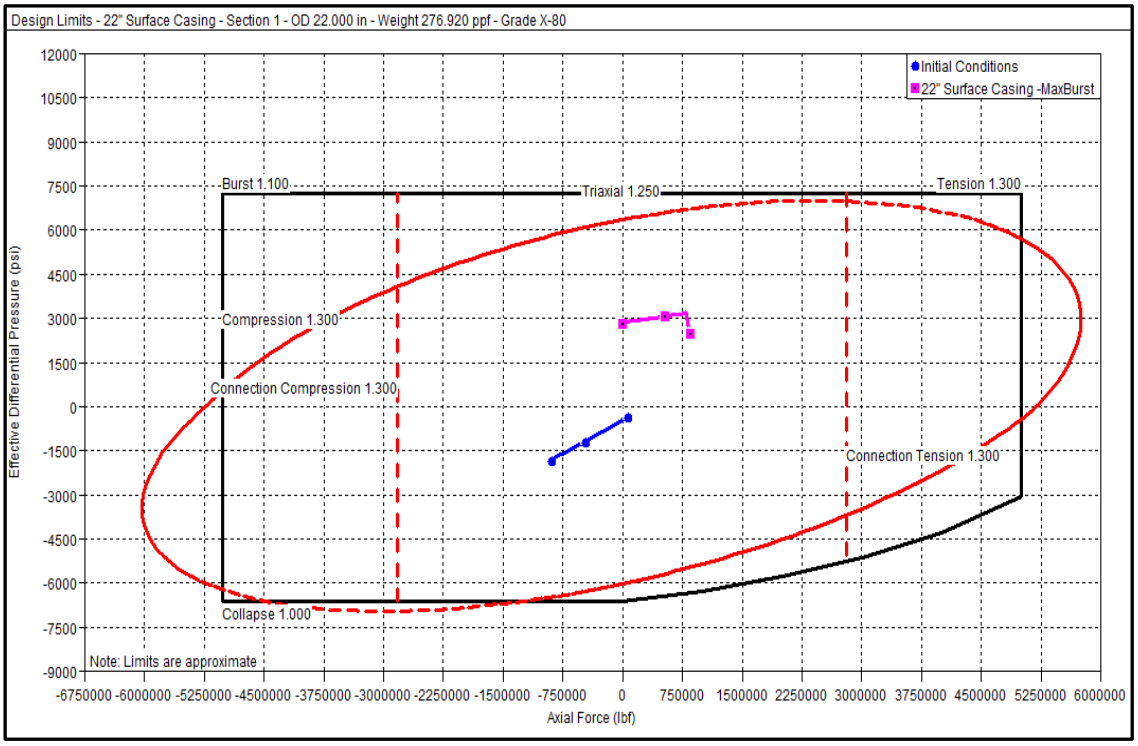

Figure 4.4 – The 22" surface casing design limits plot in a restricted flow scenario

As shown in **Figure 4.4**, the 22" surface casing's integrity is intact during the restricted flow blowout.

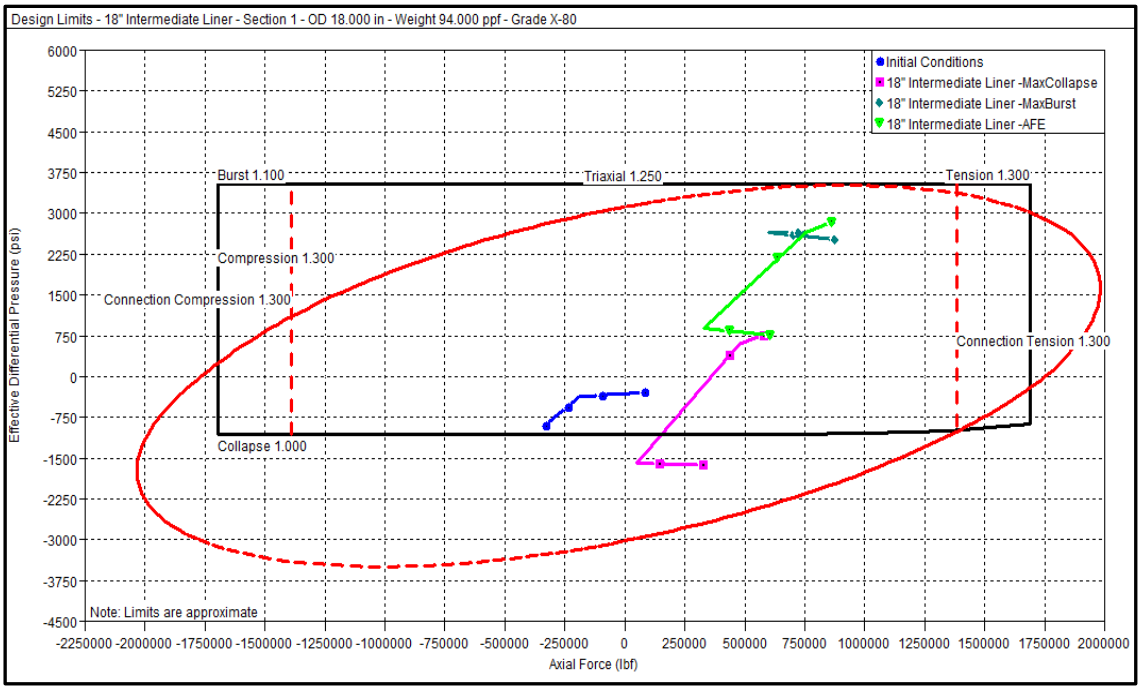

Figure 4.5 – The 18" Intermediate Liner design limits plot in a restricted flow scenario

The maximum collapse for the 18" intermediate liner exceeds the collapse safety margin; however, as shown in **Figure 4.5**, the string does not fail under the applied pressure.

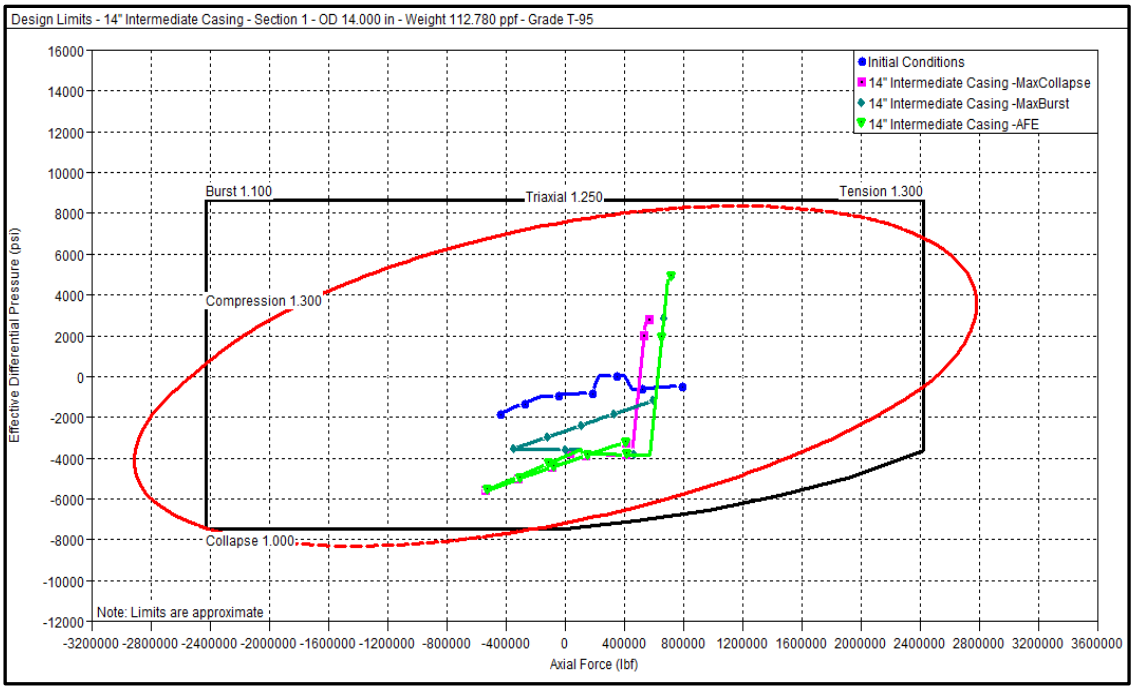

Figure 4.6 – The 14" intermediate casing design limits plot in a restricted flow scenario

Figure 4.6 shows that the collapse, burst, and AFE for the 14" intermediate casing all fall within the safe design limits.

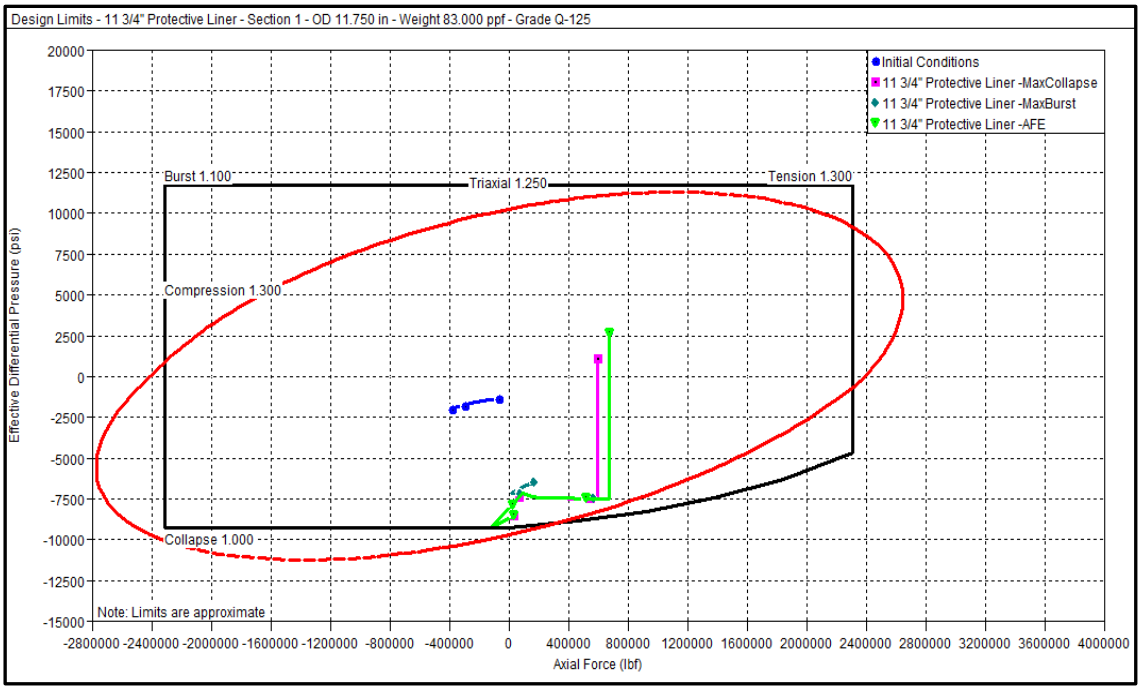

Figure 4.7 – The 11 ¾" protective liner design limits plot in a restricted flow scenario

Similar to the 14" intermediate casing, the 11 ¾" protective liner withstands the applied forces during the restricted flow of hydrocarbons throughout the wellbore (see **Figure 4.7**).

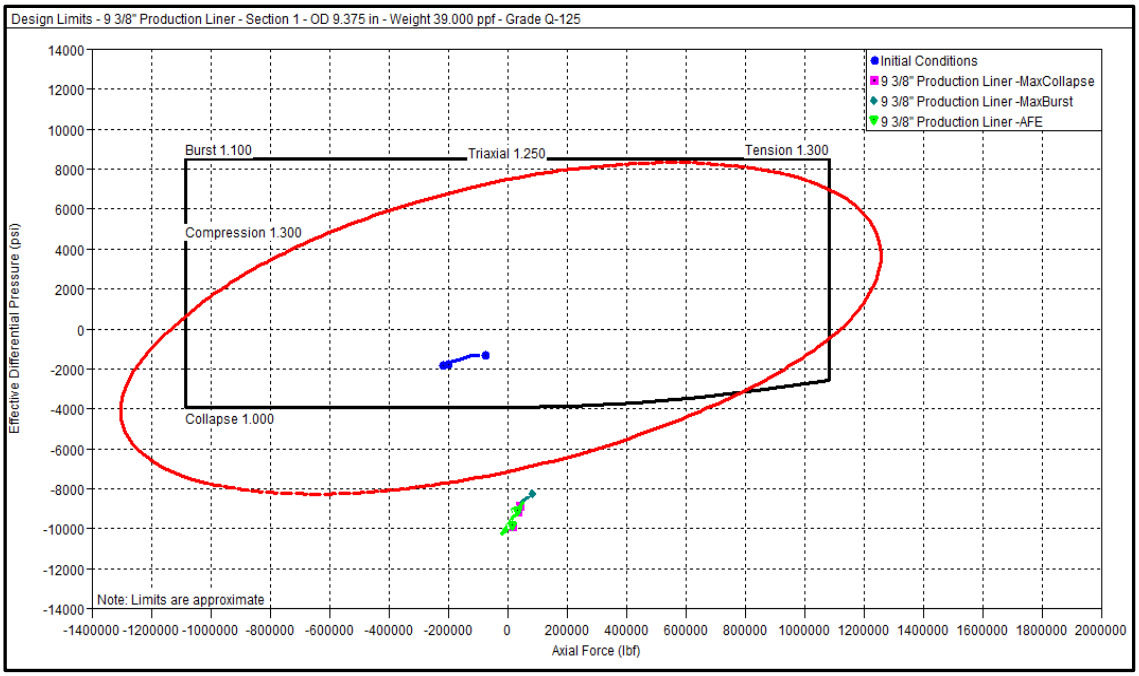

Figure 4.8 – The 9 ⅜" production liner design limits plot in a restricted flow scenario

The 9 ⅜" production liner is designed to collapse in the case of an uncontrolled flow to a seabed. The reason for such a design is that if the well needs to be shut in, the wellbore shut-in pressure should not exceed the pressure rating of the BOP at the seabed. The BOP stack is rated at 10K psi. As **Figure 4.9** illustrates, with no collapse at the 9 ⅜" shoe, the shut-in pressure is 12,500 psi which is higher than the limit. However, if the 9 ⅜" collapses, the 11 ¾" shoe will be exposed which will result in an underground venting into the shoe. The shut-in pressure then will stabilize at 9,500 psi.

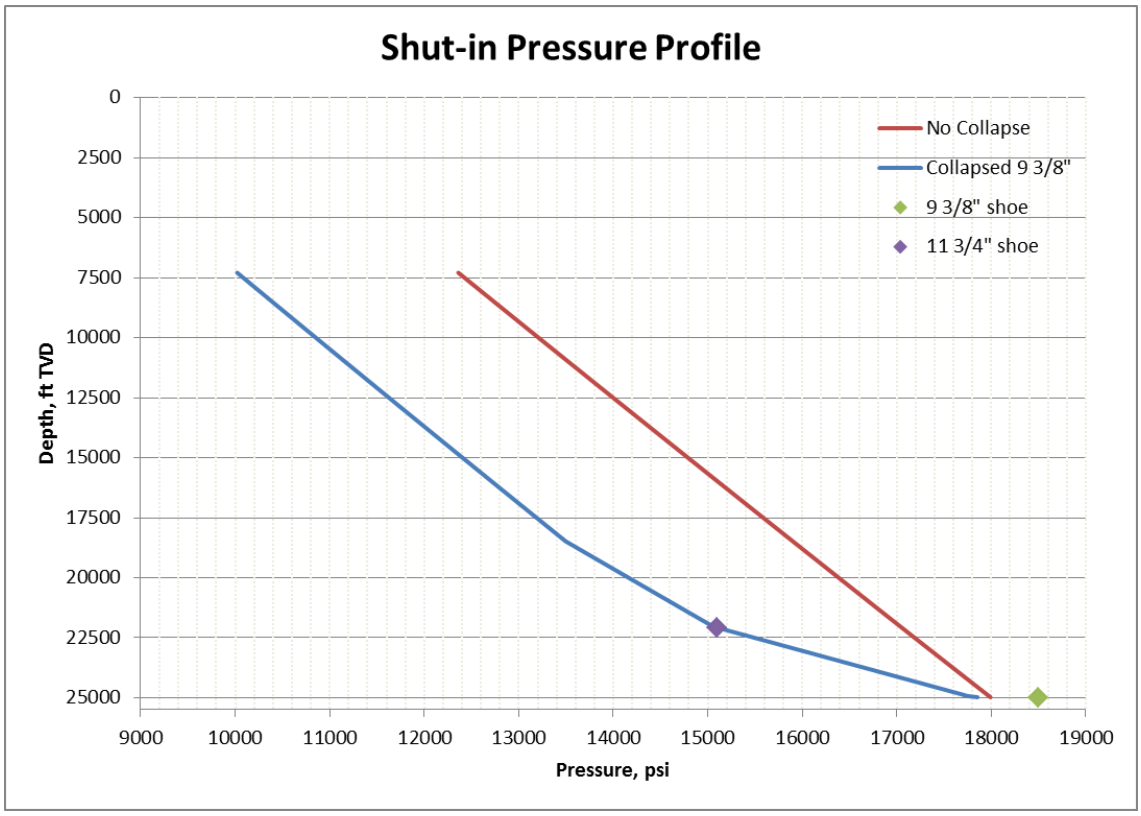

Figure 4.9 – Wellbore shut-in pressure profile versus the integrity of the 9 ⅜" liner

Now that the design limits for the restricted flow have been probed, it can be concluded that the wellbore integrity will not be compromised in the case of an uncontrolled flow to the seabed. However, as will be presented below, the design limits for a case of WCD should be investigated to confirm the conclusion.

4.2.2 WCD Scenario

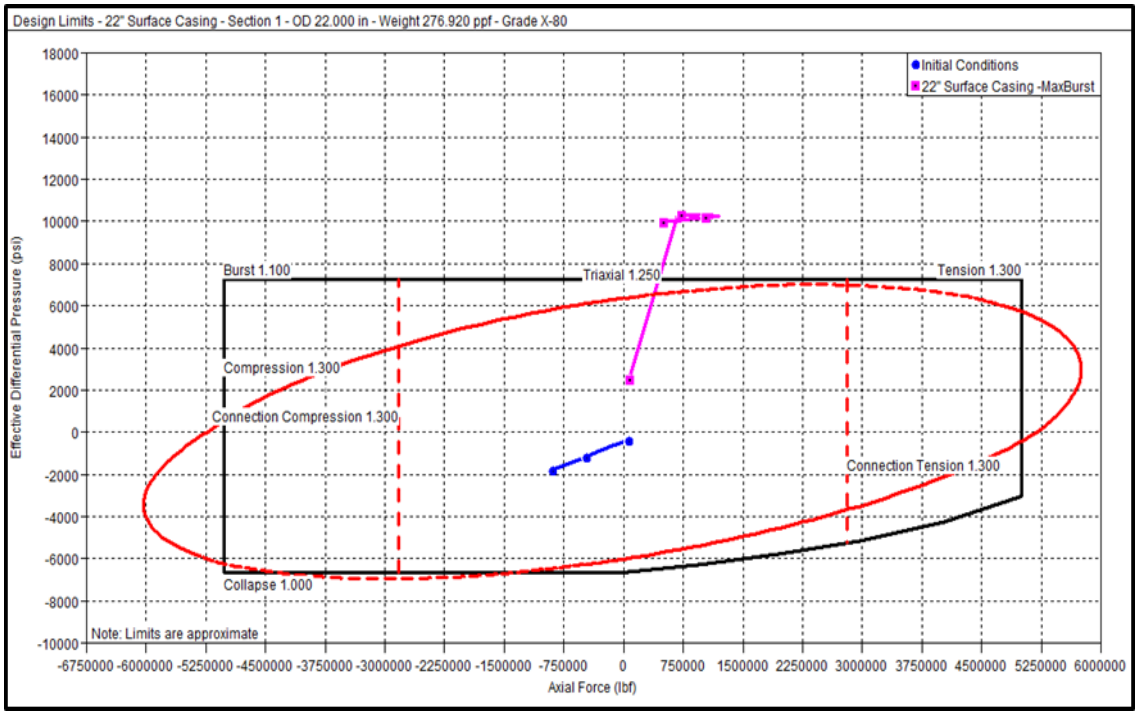

Figure 4.10 - The 22" surface casing design limits in a WCD scenario

As **Figure 4.10** depicts, the burst loading at the 22" surface casing exceeds the limit; however, since the 22" casing is fully cemented, this should not raise an issue.

The burst of the 18" liner (see **Figure 4.11**) was caused by the collapse of the 14" casing (see **Figure 4.12).**

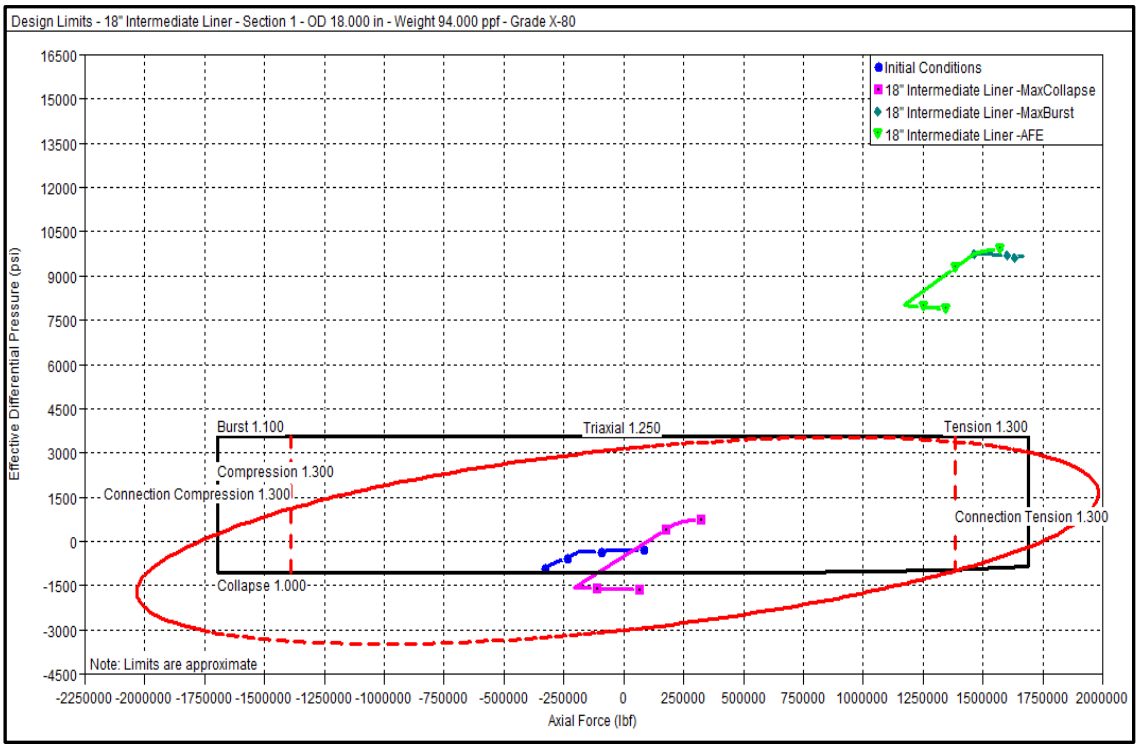

Figure 4.11 – The 18" Intermediate Liner design limits in a WCD scenario

As **Figure 4.12** shows, unlike the restricted flow scenario, the 14" intermediate casing collapses under the forces exerted by the annular pressure build up.

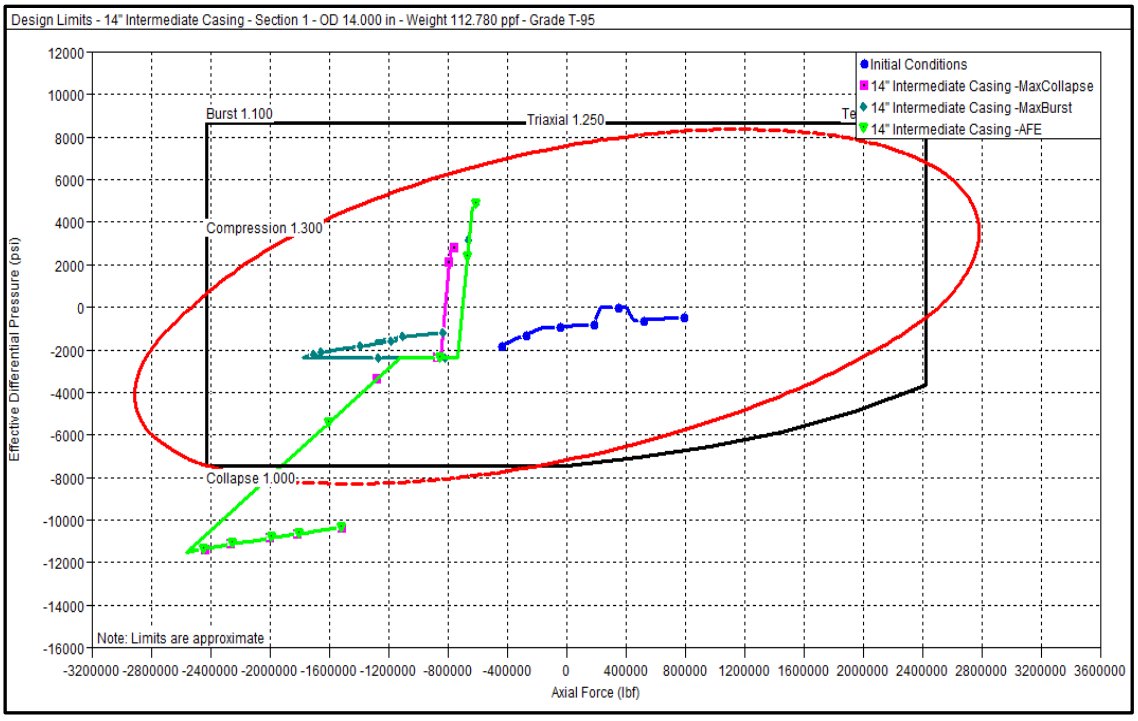

Figure 4.12 - The 14" intermediate casing design limits plot at WCD

Although the 11 ¾" protective liner does not fail (see Figure 4.13), the loss of integrity of the other two strings could potentially yield broaching and a total loss of well integrity.

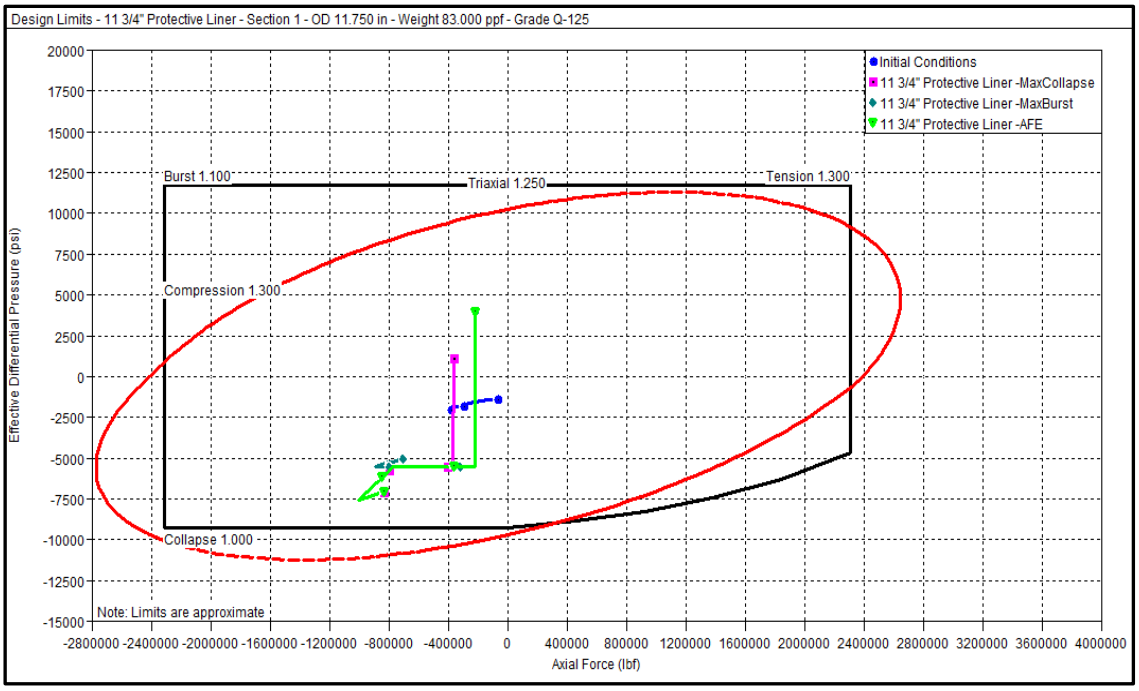

Figure 4.13 - 11 ¾" protective liner design limits plot at WCD

Similar to the case of restricted flow, the collapse of the 9 ⅜" production liner (see **Figure 4.14**) will not be an issue.

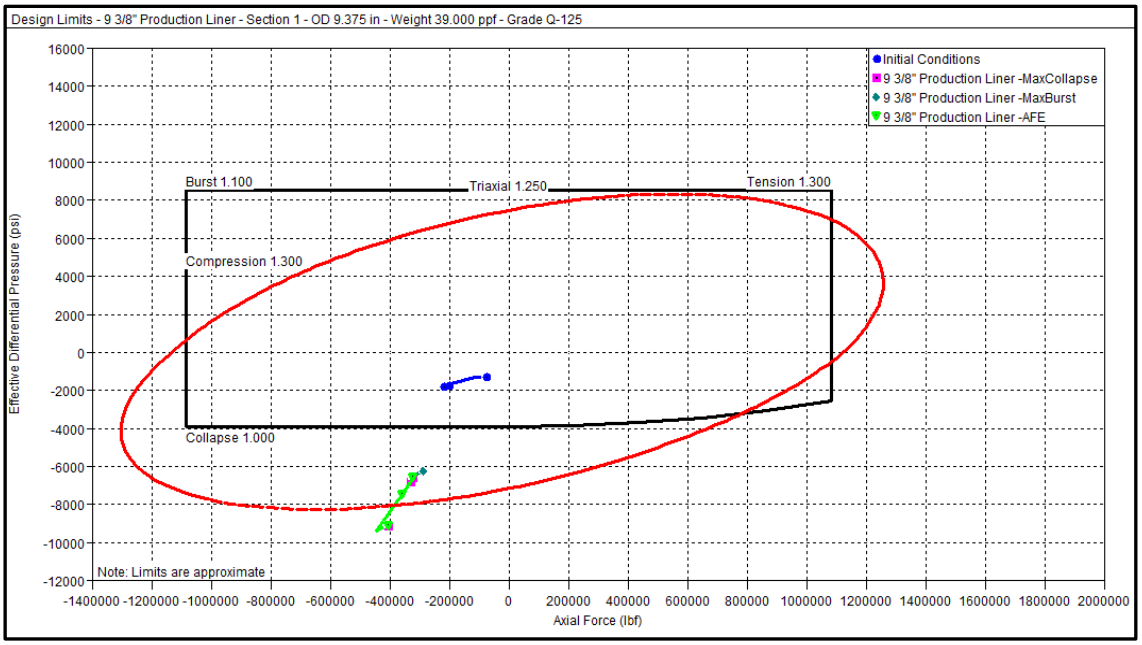

Figure 4.14 – 9 ⅜" production liner design limits at WCD

Even though an examination of the design limits in a case of restricted flow did not reveal any issues with the planned design, it can be concluded that the results of the WCD helped to identify design flaws that could lead to a total loss of wellbore integrity.

4.2.3 Alternate Design

To resolve the discussed APB issues, an alternative well design (as shown in **Figure 4.15)** is proposed as follows:

1. The 14" intermediate casing should be substituted by a 16" protective liner.
2. The 11 ¾" protective liner should be substituted by 12 ¼" intermediate casing.

3. The 9 ⅜" production liner should be substituted by 8 ⅝" production liner.

The only downside of the proposed design is that the 8 ⅝" production liner is not designed to collapse; thus, the 10K stack needs to be replaced by a 15K stack. The design limits for a WCD are evaluated for the proposed design and presented in the next section.

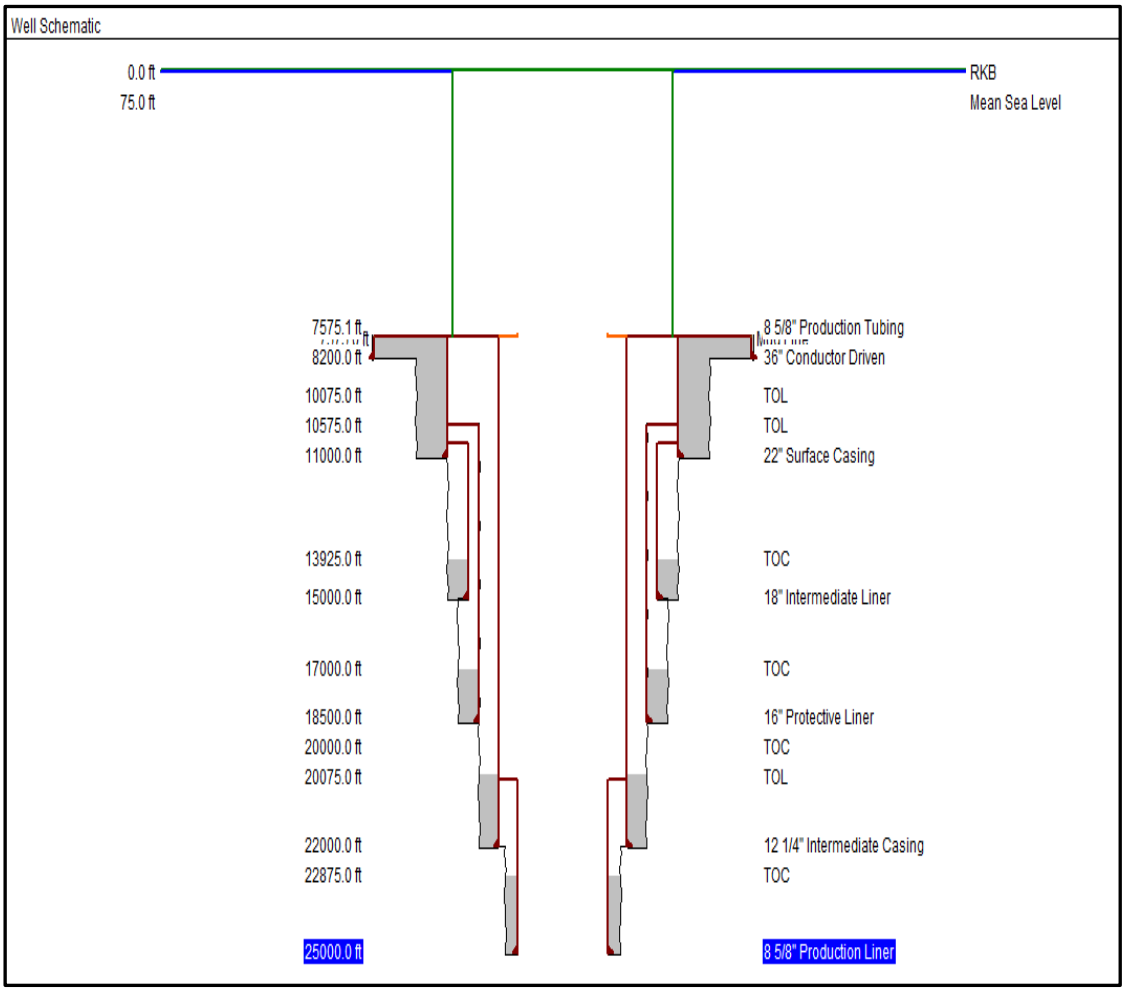

Figure 4.15 – Alternative design to prevent casing failure in a WCD scenario

The increase in the pressure and volume of the trapped annular fluids attributable to the APB are shown in **Table 4.2**. Note that the AFE in the strings is even higher than in the case previously discussed.

Table 4.2 – Annular Fluid Expansion (AFE) of WCD scenarios for the alternate well design

Case	String Annulus	Incremental AFE Volume, bbl	Incremental AFE Pressure, psi
WCD	18" Intermediate Liner	46.5	1,768
	16" Protective Liner	43.0	3,363
	12 ¼" Intermediate Casing	93.1	6,738
	8 ⅝" Production Liner	2.7	2,929

Similar to the original design, a burst of the fully cemented 22" surface casing should not pose a problem (see **Figure 4.16**).

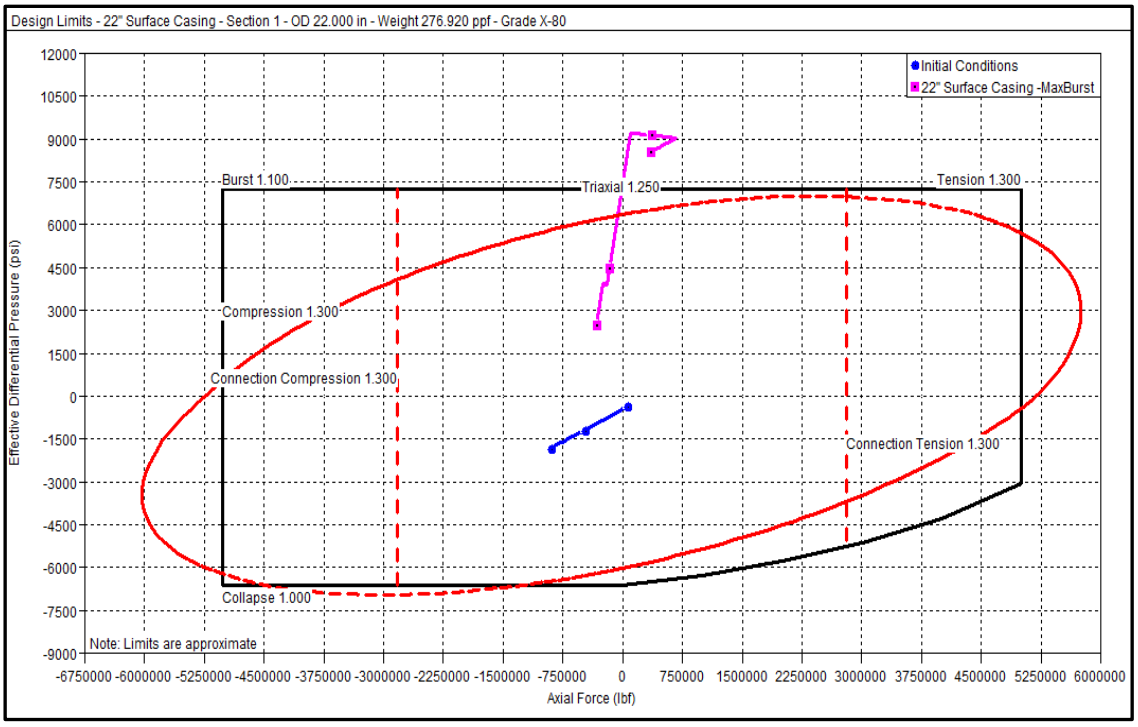

Figure 4.16 – The 22" surface casing alternative design limits plot at WCD

The maximum collapse for the 18" intermediate liner exceeds the collapse safety margin; however, unlike the original design, the string does not burst (see **Figure 4.17**).

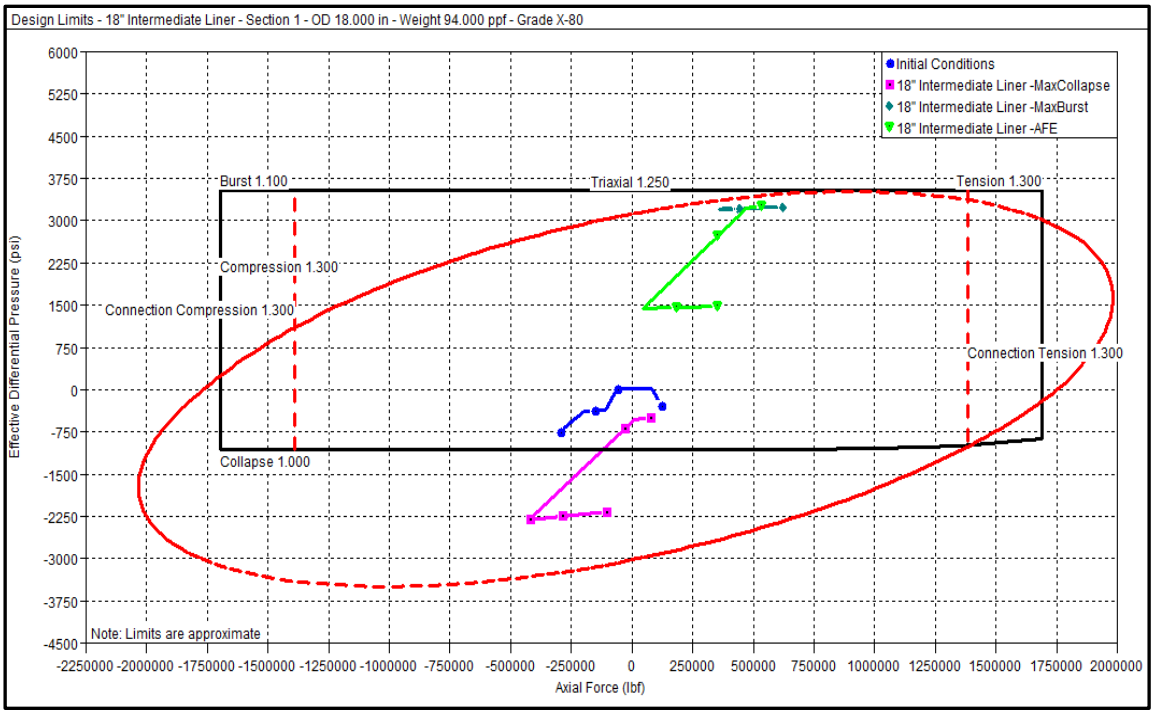

Figure 4.17 – The 18" intermediate liner alternative design limits plot at WCD

Although the 16" protective liner bursts (see **Figure 4.18**), since the integrity of the 12 ¼" is not compromised (see **Figure 4.19**), the loss of the 16" liner is acceptable.

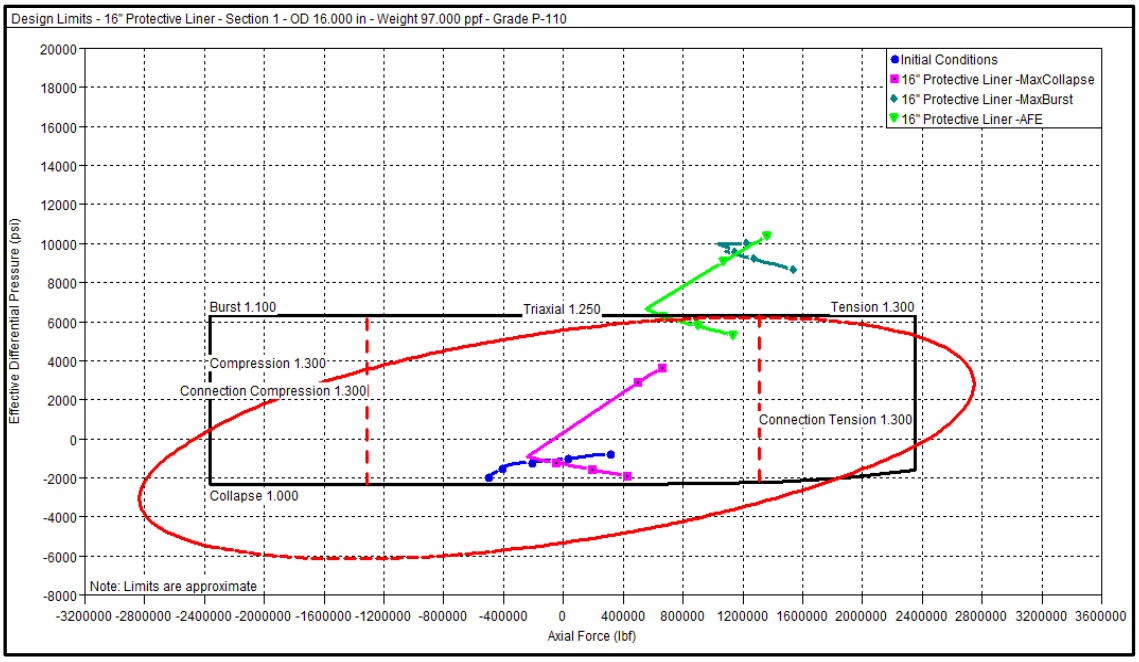

Figure 4.18 - The 16" protective liner alternative design limits plot at WCD

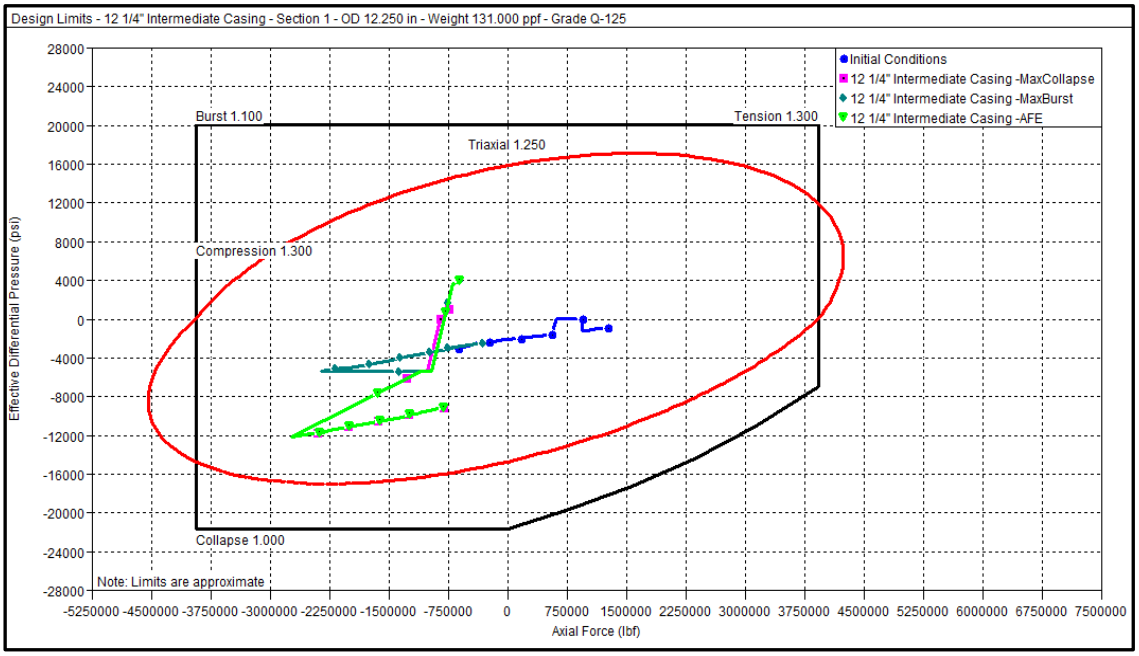

Figure 4.19 – The 12 ¼" intermediate casing alternative design limits plot at WCD

As planned, the 8 ⅝" production liner does not fail.

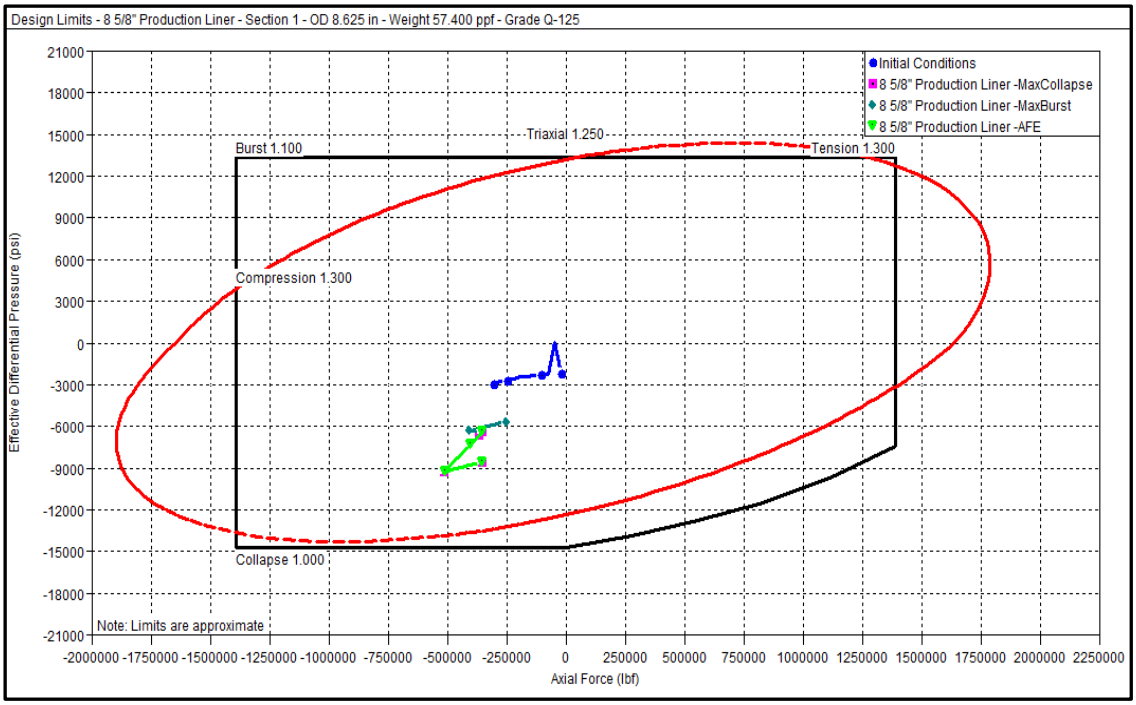

Figure 4.20 – The 8 ⅝" production liner new design limits plot at WCD

5 CONCLUSIONS AND FUTURE WORK

5.1 Conclusions

The following conclusions can be drawn from this study:

1. The dynamic interaction of fluid flow and tubular systems within an HPHT well must be analyzed by coupling a transient multiphase flow model and a robust transient tubular load/stress analysis model. The lack of such a unified solution/software package in the industry could result in the loss of the well, an environmental disaster, or worse, loss of lives.
2. The proposed new methodology in this study could potentially prevent unforeseen well integrity issues.
3. The flowing pressure and temperature profiles predicted by the WELLCAT™'s built-in flow models could significantly deviate from the actual values. It is very important to tune and validate those models with a transient nodal analysis multiphase model such as OLGA.
4. The fluid's physical and thermal properties should be determined with an appropriate EoS, which might also need a regression analysis. In such cases, PVTsim or similar PVT analysis packages need to be used to calculate the fluid properties.
5. It is strongly recommended to check the wellbore design for both the restricted flow and WCD scenarios. This is because the very different prevailing flow conditions of each scenario could yield completely different conclusions.

5.2 Future Work

Future work in this area should include but not be limited to:

1. Continuing research on different blowout conditions that could lead to cases with extreme differential pressures. Factors such as wellbore inclination, water depth, long string casing design, crossflow between production intervals, and simultaneous production of gas and water could all be investigated.
2. Evaluating wellbore integrity during capping operations and comparing the hard and soft shut-ins with a controlled flow to the surface.
3. Performing comprehensive sensitivity analyses on different types of spacers and completion fluids.
4. Developing software packages that can dynamically analyze the transient effects of fluid flow and tubular loads.

REFERENCES

Adams, A. 1991. How to Design for Annulus Fluid Heat-Up. Paper SPE 22871 presented at the Annual Technical Conference and Exhibition, Dallas, TX, 6-9 October.

Adams A.J. and MacEachran, A. 1994. Impact on Casing Design of Thermal Expansion of Fluids in Confined Annuli. *SPEDC* **9**(3): 210-216. SPE-21911-PA.

Ansari, A.M., Sylvester, N. D., Sarica, C., Shoham, O. and Brill, J.P. 1994. A Comprehensive Mechanistic Model for Upward Two-Phase Flow in Wellbores. *SPE J Prod & Fac* (May): 143-152.

API Bulletin 5C3. 1985. Bulletin for Formulas and Calculations for Casing, Tubing, Drillpipe, and Line Pipe Properties. Fourth edition, Dallas, TX.

Barnea, D., Shoham, O. and Taitel, Y. 1980. Flow Pattern Transition for Gas-Liquid Flow in Horizontal and Inclined Pipes. International Journal of Multiphase Flow 6(3): 217-225.

Beggs, D.H. and Brill, J.P. 1973. A Study of Two-Phase Flow in Inclined Pipes. JPT 25(5): 607-617.

Bloys, B., Gonzalez, M., Hermes, R., Bland, R., Foley, R., Tijerina, R., Davis, J., Cassel, T., Daniel, J., Robinson, I. and Eley, R. 2007. Trapped Annular Pressure Mitigation – A Spacer Fluid that Shrinks. Paper SPE/IADC 104698 presented at the SPE/IADC Drilling Conference, Amsterdam, Netherlands, 20-22 February.

Bradford, D.W., Fritcjie, D.G., Gibson, D.H., Gosch, S.W., Pattillo, P.D., Sharp, J.W. and Taytor, C.E. 2002. Marlin Failure Analysis and Redesign: Part 1- Description of Failure. Paper SPE 88814 presented at the IADC/SPE Drilling Conference, Dallas, TX, 26-28 February.

Crandall, S.H. and Dahl, N.C. 1959. An Introduction to the Mechanics of Solids, New York City, NY: McGraw-Hill Book Company.

Duns, H. and Ros, N.C.J. 1963. Vertical flow of gas and liquid mixtures in wells. Paper SPE 10132 presented at the World Petroleum Congress, Frankfurt, Germany, 19-26 June.

Gray, H.E. 1974. Vertical Flow Correlation in Gas Wells. API Manual 14B, Appendix B, Dallas, TX.

Hagedorn, A.R. and Brown, K.E. 1965. Experimental Study of Pressure Gradients Occurring During Continuous Two-Phase Flow in Small-Diameter Vertical Conduits. JPT 17 (April): 475-484.

Halal, A.S. and Mitchell, R.F. 1994. Casing Design for Trapped Annular Pressure Build-Up. SPEDC 9(2): 107-114. SPE-25694-PA.

Kaarstad, E., Aadony, B.S. and Simonsen J. 2008. Trapped Annular Pressure Data and Analysis. Paper IPTC 12675 presented at the IPTC conference, Kuala Lumpur, Malaysia, 3-5 December.

Kaya, A.S., Sarica, C. and Brill, J. P. 1999. Comprehensive Mechanistic Modeling of Two-Phase Flow in Deviated Wells. Paper SPE 56522 presented at the SPE Annual Technical Conference and Exhibition, Houston, TX, 3-6 October.

Klementich, E.F. and Jellison, M.J. 1986. A Service-Life Model for Casing String. SPEDE 1(2): 141-152. SPE-12361-PA.

Orkiszewski, J. 1967. Predicting Two-Phase Pressure Drops in Vertical Pipe. JPT 19(6): 829-838.

Peng, D.Y. and Robinson, D.B. 1976. A New Two-Constant Equation of State. Industrial and Engineering Chemistry: Fundamentals, 15(1): 59–64.

Sathuvalli, U.B., Payne M.L., Patillo, P.D., Rahman, S. and Suryanarayana P.V. 2005. Development of a Screening System to Identify Deepwater Wells at Risk for Annular Pressure Buildup. Paper SPE 92594 presented at the SPE/IADC Drilling Conference, Amsterdam, Netherlands, 23-25 February.

Soave, G. 1972. Equilibrium Constants from a Modified Redlich-Kwong Equation of State. Chemical Engineering Science, 27(6): 1197-1203.

Zhang, H.Q., Wang, Q., Sarica, C. and Brill, J.P. 2003. A Unified Mechanistic Model for Slug Liquid Holdup and Transition between Slug and Dispersed Bubble Flows. International Journal of Multiphase Flow, 29 (January): 97-107.

APPENDIX A

The subject well is a vertical well with a TD of 25,000 ft at a water depth of 7,500 ft. The pressure and the temperature at the TD of the well are 18,000 psi and 375 oF, respectively.

The blowout simulation was run with the inflow performance relation (IPR) as the inlet condition. Blowout rates have been calculated for a blowout through the open hole to the seabed. A backpressure of 3,230 psi was used as the outlet condition for the discharge to seabed scenario. The flow rates reported below reflect the blowout rates in standard conditions (14.65 psi, and 59 °F) after a single-stage flash of the reservoir fluid.

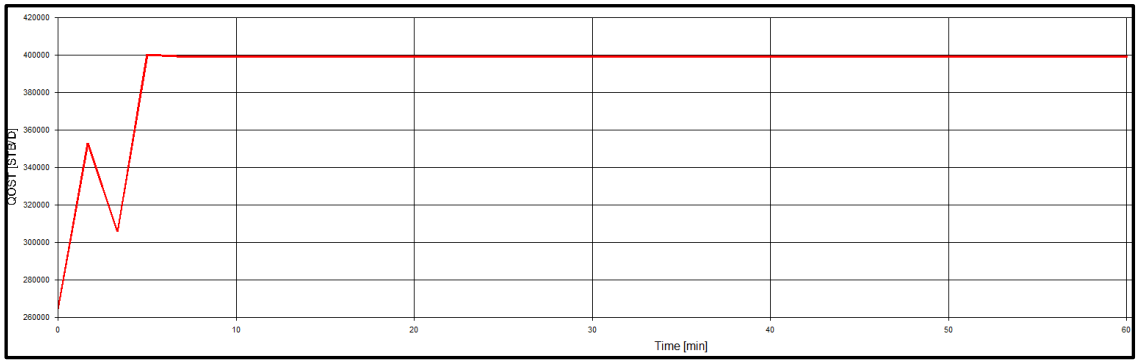

Figure A1 – WCD predicted by OLGA

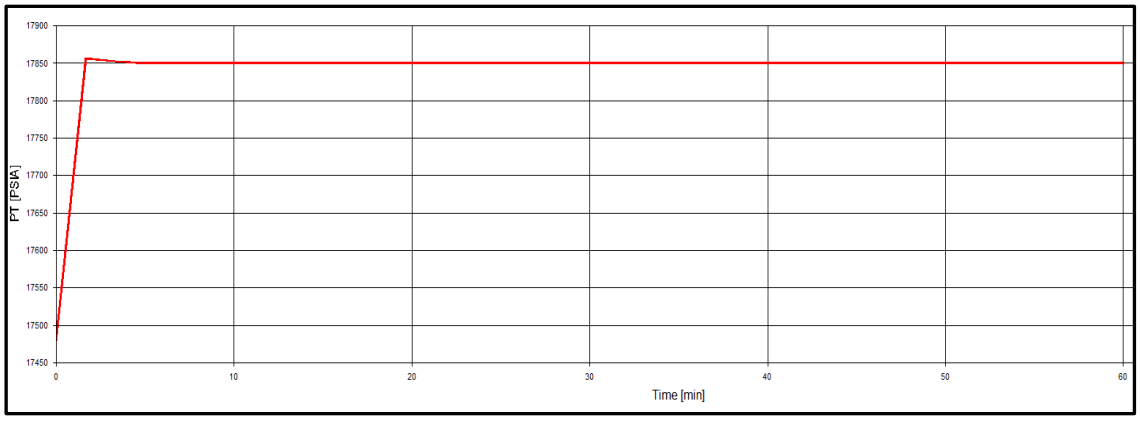

Figure A2 – Flowing Bottomhole Pressure Predicted by OLGA

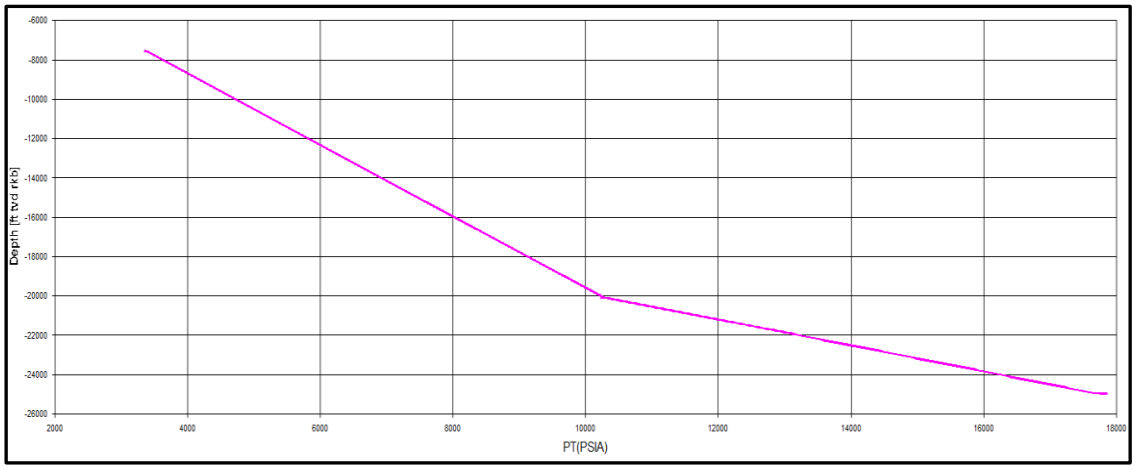

Figure A3 – Flowing Pressure Profile Predicted by OLGA

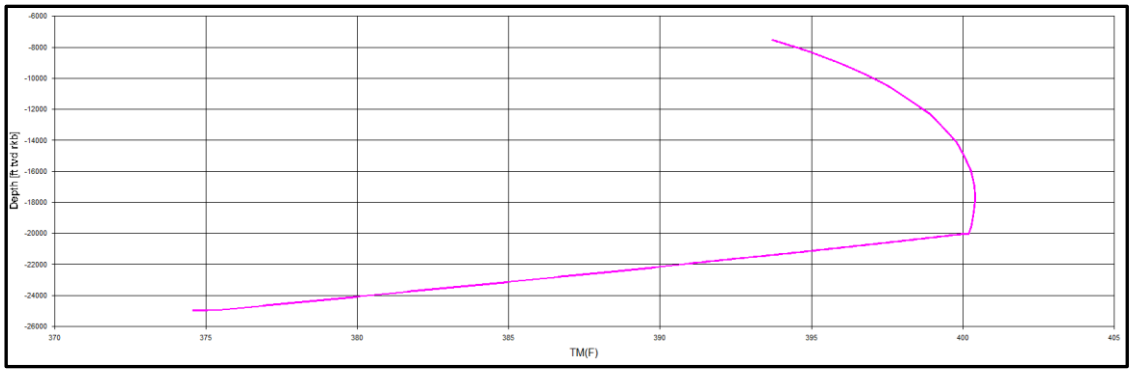

Figure A4 – Flowing Temperature Profile Predicted by OLGA

Table A1 – Blowout rates

Blowout scenario	FBHP at top of sand, psi	Gas rate, MMSCFD	Oil rate, bpd
WCD	17,500	275	400,000
Restricted flow	8,500	27.5	40,000

The WCD scenario is defined as a blowout through the open hole to the seabed with full reservoir exposure and no flow restrictions. The restricted flow scenario is based on partial penetration into the top of the reservoir.

MultiString Annular Fluid Expansion Summary

	String Annulus	Region	Incremental AFE Pressure (1) (psi)	Incremental AFE Volume (2) (bbl)
1	18" Intermediate Liner	Region 1	1768.00	46.5
2	16" Protective Liner	Region 1	3363.00	43.0
3	12 1/4" Intermediate Casing	Region 1	6738.00	93.1
4	8 5/8" Production Liner	Region 1	2929.00	2.7
5				
6	(1) Pressure change caused solely by the Annular Fluid Expansion (AFE) phenomenon.			
7	(2) Volume change caused solely by the Annular Fluid Expansion (AFE) effect.			

Figure A5 – The AFE Table for Alternate Design

APPENDIX B

The fluid composition is provided in Table B1. The PR78 Peneloux EoS is used to characterize the fluid, and then regression analysis is used to tune the properties and match them with the values measured at the PVT laboratory.

Table B1 – Characterized fluid composition

Component	Mole %	Mole Weight	Density, lb^3/ft
N2	1.65	28.014	
CO2	0.495	44.01	
C1	29.217	16.043	
C2	8.694	30.07	
C3	6.652	44.097	
iC4	1.227	58.124	
nC4	3.878	58.124	
iC5	1.588	72.151	
nC5	2.424	72.151	
C6	3.476	86.178	41.4522
C7	3.032	96	46.0718
C8	3.445	107	47.7574
C9	2.898	121	48.7562
C10-C11	8.233	140.006	50.102
C12	3.265	161	51.317
C13-C14	5.211	181.929	52.3457
C15-C16	3.841	213.391	53.5779
C17-C18	2.832	243.467	54.6586
C19-C20	2.088	268.544	55.6226
C21-C24	2.673	308.729	56.8441
C25-C29	1.697	369.281	58.4446
C30-C80	1.484	500.707	61.2024

All properties in standard conditions are based on a single stage flash (modeled using PVTsim v20.0.0).

Table B2 – Reservoir properties

Properties	**@ Standard Conditions 14.65 psi and 59 °F**	**@ Downhole Conditions 18,000 psi and 375 °F**
GOR, scf/STB	685	Oil only
Oil density, °API	36.9	56.6
Oil viscosity, cp	3.5	0.4
Gas viscosity, cp	0.01	-
FVF, bbl/STB	-	1.32
Saturation pressure, psi	2,500 psi at 375 °F	

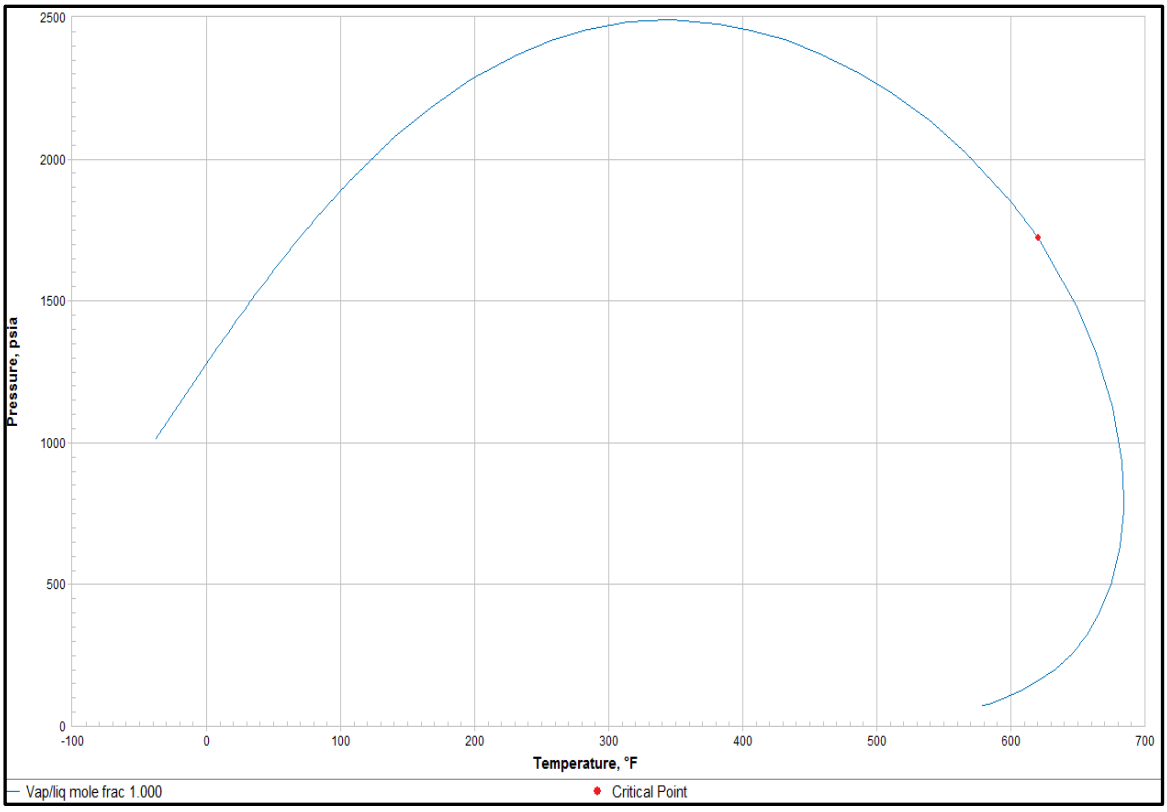

Figure B1 – Phase envelope